

1 The STING ligand 2'3'-cGAMP induces an NF- κ B-dependent anti-bacterial innate
2 immune response in the starlet sea anemone *Nematostella vectensis*
3

4 Shally R. Margolis¹, Peter A. Dietzen¹, Beth M. Hayes², Stephen C. Wilson^{1,3}, Brenna C.
5 Remick¹, Seemay Chou^{2,4}, Russell E. Vance^{1,5,6*}
6
7

8 ¹ Division of Immunology and Pathogenesis, Department of Molecular and Cell Biology,
9 University of California, Berkeley, CA 94720 USA

10 ² Department of Biochemistry and Biophysics, University of California, San Francisco,
11 San Francisco, CA 94158, USA.

12 ³ Current Address: Bristol Myers Squibb, 200 Cambridgepark Dr., Cambridge, MA
13 02140

14 ⁴ Chan Zuckerberg Biohub, San Francisco, CA

15 ⁵ Cancer Research Laboratory and the Immunotherapeutics and Vaccine Research
16 Initiative, University of California, Berkeley, CA 94720

17 ⁶ Howard Hughes Medical Institute, University of California, Berkeley, CA 94720

18 * correspondence: rvance@berkeley.edu
19

20 **Author Contributions:** S.R.M., P.A.D., B.M.H., S.C.W., S.C. and R.E.V. designed
21 research; S.R.M., P.A.D., B.M.H., S.C.W., and B.C.R. performed research; S.R.M.,
22 P.A.D., and B.M.H. analyzed data; S.R.M. and R.E.V. wrote the paper; and P.A.D.,
23 B.M.H., S.C.W, and S.C. provided critical review.

24 **Competing Interest Statement:** R.E.V. consults for Ventus Therapeutics. The other
25 authors declare no competing interests.

26 **Classification:** Biological Sciences; Immunology and Inflammation

27 **Keywords:** STING, Cnidaria, *Nematostella vectensis*, NF- κ B, innate immunity

28 **Abstract**

29 In mammals, the cGAS-cGAMP-STING pathway is crucial for sensing viral
30 infection and initiating an anti-viral type I interferon response. cGAS and STING are
31 highly conserved genes that originated in bacteria and are present in most animals. By
32 contrast, interferons only emerged in vertebrates; thus, the function of STING in
33 invertebrates is unclear. Here, we use the STING ligand 2'3'-cGAMP to activate immune
34 responses in a model cnidarian invertebrate, the starlet sea anemone *Nematostella*
35 *vectensis*. Using RNA-Seq, we found that 2'3'-cGAMP induces robust transcription of
36 both anti-viral and anti-bacterial genes, including the conserved transcription factor NF-
37 κ B. Knockdown experiments identified a role for NF- κ B in specifically inducing anti-
38 bacterial genes downstream of 2'3'-cGAMP, and some of these genes were also found
39 to be induced during *Pseudomonas aeruginosa* infection. Furthermore, we
40 characterized the protein product of one of the putative anti-bacterial genes, the *N.*
41 *vectensis* homolog of Dae4, and found that it has conserved anti-bacterial activity. This
42 work describes an unexpected role of a cGAMP sensing pathway in anti-bacterial
43 immunity and suggests that a broad transcriptional response is an evolutionarily
44 ancestral output of 2'3'-cGAMP signaling in animals.

45
46 **Significance statement**

47 Anti-viral immune responses are initiated via signaling pathways such as the
48 STING pathway. In mammals, activation of this pathway results in the production of
49 anti-viral molecules called interferons. Surprisingly, the STING pathway is present in
50 organisms such as sea anemones that lack interferons; the function of this pathway in
51 these organisms is thus unclear. Here we report that in the anemone *Nematostella*
52 *vectensis*, a small molecule activator of the STING pathway, cGAMP, not only induces
53 an anti-viral response, but also stimulates an anti-bacterial immune response. These
54 results provide insights into the evolutionary origins of innate immunity, and suggest a
55 broader ancestral role for cGAMP-STING signaling that evolved toward more
56 specialized anti-viral functions in mammals.

57 Introduction

58 The innate immune system is an evolutionarily ancient system that detects
59 pathogens and initiates their elimination. In mammals, the cGAS-STING pathway is
60 critical for sensing and responding to intracellular DNA, which is particularly important
61 for innate responses to DNA viruses (1, 2). The sensor protein in this pathway, cyclic-
62 GMP-AMP synthase (cGAS), is an enzyme that binds directly to cytosolic DNA and
63 produces 2'3'-cGAMP, a cyclic dinucleotide (CDN) second messenger that binds and
64 activates STING (3-8). Active STING uses its C-terminal tail (CTT) to recruit TBK1,
65 which then phosphorylates and activates the transcription factor IRF3 to induce the
66 expression of type I interferons (IFNs) (9-12). Type I IFNs are secreted cytokines that
67 signal via JAK-STAT signaling to induce transcription of hundreds of anti-viral genes
68 known as interferon-stimulated genes (ISGs) (13, 14). STING also activates NF- κ B,
69 MAP kinase (15), STAT6 (16), and autophagy-like pathways (17-20), as well as
70 senescence (21) and cell death (22-26), although the mechanism of activation of these
71 pathways, and their importance during infection, are less well understood.

72 Type I IFNs are thought to be a relatively recent evolutionary innovation, with
73 identifiable interferon genes found only in vertebrates (27). In contrast, STING and
74 cGAS are conserved in the genomes of most animals and some unicellular
75 choanoflagellates. Remarkably, CDN to STING signaling seems to have originated in
76 bacteria, where it may be important in bacteriophage defense (28, 29). Studies on the
77 function of STING in animals that lack type I IFN have been mostly limited to insects,
78 where STING seems to be protective during viral (30-33), bacterial (34), and
79 microsporidial (35) infection. In insects, STING may promote defense through activation
80 of autophagy (32, 35) and/or induction of NF- κ B-dependent defense genes (30, 31, 34);
81 however, the biochemical mechanisms of STING activation in insects remain poorly
82 understood. Biochemically, perhaps the best-characterized invertebrate STING is that of
83 the starlet sea anemone, *Nematostella vectensis*, a member of one of the oldest animal
84 phyla (Cnidaria). *N. vectensis* encodes a surprisingly complex genome that harbors
85 many gene families found in vertebrates but absent in other invertebrates such as
86 *Drosophila* (36). *N. vectensis* STING (nvSTING) and human STING adopt remarkably
87 similar conformations when bound to 2'3'-cGAMP, and nvSTING binds to this ligand
88 with high affinity ($K_d < 1$ nM) (37). The *N. vectensis* genome also encodes a cGAS
89 enzyme that produces 2'3'-cGAMP in mammalian cell culture (17). In vertebrates,
90 STING requires its extended CTT to initiate transcriptional responses (38, 39); however,
91 nvSTING lacks an extended CTT and thus its signaling mechanism and potential for
92 inducing transcriptional responses is unclear. Based on experiments with nvSTING in
93 mammalian cell lines, CTT-independent induction of autophagy has been proposed as
94 the 'ancestral' function of STING (17), but the endogenous function of STING in *N.*
95 *vectensis* has never been described.

96 Despite the genomic identification of many predicted innate immune genes (40, 41),
97 few have been functionally characterized in *N. vectensis*. The sole *N. vectensis* Toll-like
98 receptor (TLR) is reported to bind flagellin and activate NF- κ B in human cell lines, and is
99 expressed in cnidocytes, the stinging cells that define cnidarians (42). *N. vectensis* NF-
100 κ B (nvNF- κ B) binds to conserved κ B sites, is inhibited by *N. vectensis* I κ B (43), and
101 seems to be required for the development of cnidocytes (44). However, no activators of
102 endogenous nvNF- κ B have yet been identified. Work probing the putative anti-viral
103 immune response in *N. vectensis* found that double-stranded RNA (dsRNA) injection
104 into *N. vectensis* embryos leads to transcriptional induction of genes involved in the
105 RNAi pathway as well as genes with homology to ISGs (45). This response is partially
106 dependent on a RIG-I-like receptor, indicating deep conservation of anti-viral immunity

107 (45). However, no anti-viral or anti-bacterial effectors from *N. vectensis* have been
108 functionally tested.

109 Here, we characterize the response of *N. vectensis* to 2'3'-cGAMP stimulation.
110 Similar to the response of vertebrates to 2'3'-cGAMP, we find robust transcriptional
111 induction of putative anti-viral genes with homology to vertebrate ISGs. In addition, we
112 observed induction of numerous anti-bacterial genes that are not induced during the
113 vertebrate response to 2'3'-cGAMP. We found a selective requirement for $\text{nvNF-}\kappa\text{B}$ in
114 the induction of some of the anti-bacterial genes, and many of these genes are also
115 induced during *Pseudomonas aeruginosa* infection, suggesting a functional role in anti-
116 bacterial immunity. Of these induced genes, we selected and characterized the anti-
117 bacterial activity of a *Nematostella* domesticated amidase effector (*nvDae4*), a
118 peptidoglycan cleaving enzyme, and the *Nematostella* LPS- binding protein (*nvLBP*), a
119 protein that causes membrane permeabilization of *Pseudomonas aeruginosa*. This work
120 demonstrates an evolutionarily ancient role of a cGAMP-sensing pathway in the
121 transcriptional induction of anti-bacterial immunity.

122

123 Results

124 *Transcriptional response to 2'3'-cGAMP in Nematostella vectensis*

125 To assess the *in vivo* role of 2'3'-cGAMP signaling in *Nematostella vectensis*, we
126 treated 2-week-old polyps with 2'3'-cGAMP for 24 hours and performed RNA-Seq (Fig.
127 1A, Fig. S1). Thousands of genes were induced by 2'3'-cGAMP, many of which are
128 homologs of genes known to function in mammalian immunity. Despite the lack of
129 associated gene ontology (GO) terms for many of the differentially regulated genes,
130 unbiased GO term analysis revealed significant enrichment of immune-related terms
131 (Fig. 1B). We confirmed the RNA-Seq results by performing quantitative reverse
132 transcription PCR (qRT-PCR) on 48-hour-embryos treated for 4 hours with 2'3'-cGAMP
133 (Fig. 1C), and found that these genes were also induced at this early developmental
134 stage after a much shorter treatment. We also treated animals with 3'3'-linked cyclic
135 dinucleotides, which are thought to be produced exclusively by bacteria, and which also
136 bind to *nvSTING in vitro*, albeit at lower affinity (37). Both 3'3'-cGAMP and cyclic-di-
137 AMP treatment also induced some smaller number of genes, although all of these
138 genes were induced more strongly by 2'3'-cGAMP (Fig. S1). Interestingly, cyclic-di-GMP
139 treatment led to almost no transcriptional induction, despite having relatively high affinity
140 for *nvSTING in vitro*. This discrepancy may be due to differences in cell permeability
141 among different CDNs, as the ligands were added extracellularly.

142 Several interesting classes of genes were found to be upregulated in response to
143 2'3'-cGAMP. For example, several genes involved in the RNAi pathway were induced,
144 including homologs of Argonaute (*AGO2*), Dicer, and RNA-dependent RNA polymerase
145 (*Rdrp1*). In addition, many genes that are considered ISGs in mammals were also
146 induced in *N. vectensis*, including Viperin, RNase L, 2'-5'-oligoadenylate synthase
147 (*OAS*), interferon regulatory factors (*IRFs*), guanylate-binding proteins (*GBPs*), and the
148 putative pattern recognition receptors RIG-I-like receptor a (*RLRa*) and *RLRb*. These
149 results suggest a conserved role for 2'3'-cGAMP signaling in anti-viral immunity, despite
150 an apparent lack of conservation of type I interferons in *N. vectensis*. Interestingly, we
151 also found that many putative anti-bacterial genes were upregulated in response to 2'3'-
152 cGAMP, including homologs of LPS-binding protein (*LBP*), lysozyme, perforin-2, *Dae4*,
153 and mucins. These results indicate that 2'3'-cGAMP stimulation leads to a broad
154 immune response in *N. vectensis*.

155 To determine whether 2'3'-cGAMP signaled via *nvSTING* to induce these genes,
156 we injected shRNAs targeting *nvSTING* into 1-cell embryos and treated with 2'3'-

157 cGAMP 48 hours later. We extracted RNA and performed RNA-Seq on these samples,
158 and surprisingly, while nvSTING transcripts were reduced by ~50%, there was no
159 significant impact on 2'3'-cGAMP-induced gene expression (Fig. S2A, S2B). These
160 negative results were recapitulated in numerous independent qRT-PCR and Nanostring
161 experiments using 9 different shRNAs (3 shown in Fig. S2C). There are several
162 possible explanations for the failure to observe a requirement for nvSTING in 2'3'-
163 cGAMP signaling : (1) a 2-fold reduction in STING transcript levels may not result in a
164 reduction in STING protein levels if the protein is very stable; (2) even if STING protein
165 levels are reduced 2-fold, the reduction may not affect STING signaling due to threshold
166 effects; or (3) nvSTING may not be required for signaling downstream of 2'3'-cGAMP
167 due the presence of a redundant 2'3'-cGAMP sensor in *N. vectensis*. We generated an
168 anti-nvSTING antibody to validate knockdown efficiency at the protein level, but this
169 reagent did not appear to specifically detect nvSTING in anemone lysates. We also
170 tested whether an nvSTING translation-blocking morpholino could inhibit induction of
171 genes in response to 2'3'-cGAMP, but this also had no effect (Fig. S2D). Lastly, we
172 made multiple attempts to generate nvSTING mutant animals using CRISPR, using
173 multiple different guide RNAs, but the inefficiency of CRISPR in this organism and
174 issues with mosaicism prevented the generation of nvSTING null animals. We
175 previously solved the crystal structure of nvSTING bound to 2'3'-cGAMP and showed
176 that binding occurs with high affinity ($K_d < 1\text{nM}$) and in a similar mode as compared to
177 vertebrate STING (37). In addition, we found that when expressed in mammalian cells,
178 nvSTING forms puncta only in the presence of 2'3'-cGAMP, indicating some functional
179 change induced by this ligand (Fig. S2E). Thus, we hypothesize that 2'3'-cGAMP
180 signals via nvSTING, but technical issues and possible redundancy with additional
181 sensors prevent formal experimental evidence for this hypothesis.

182

183 *The N. vectensis NF- κ B homolog plays a role in the 2'3'-cGAMP response*

184 We next tested the role of conserved transcription factors that are known to
185 function downstream of STING mammals in the *N. vectensis* response to 2'3'-cGAMP.
186 Interestingly, many of these transcription factors are themselves transcriptionally
187 induced by 2'3'-cGAMP in *N. vectensis* (Fig. 1A). In mammals, the transcription factors
188 IRF3 and IRF7 induce type I IFN downstream of STING activation. While the specific
189 function of these IRFs in interferon induction are thought to have arisen in vertebrates,
190 other IRF family members, with conserved DNA binding residues, are present in *N.*
191 *vectensis* (Fig. S3). We microinjected 1-cell embryos with short hairpin RNAs (shRNAs)
192 targeting each of the 5 nvIRFs or a GFP control, treated with 2'3'-cGAMP, and
193 assessed gene expression by qRT-PCR and/or Nanostring. Knockdown of IRF
194 transcripts by 40-60% did not measurably impact gene induction by 2'3'-cGAMP (Fig.
195 S4). We similarly tested the role of the single *N. vectensis* STAT gene, as mammalian
196 STATs both induce anti-viral genes downstream of Type I IFN signaling, and may even
197 be directly activated by STING (16). Similar to the nvIRFs, we did not observe a
198 significant loss of gene induction by 2'3'-cGAMP in nvSTAT knockdown embryos by
199 both RNA-Seq and Nanostring (Fig. S4). There are several explanations for these
200 findings: (1) sufficient IRF or STAT protein may remain in knockdown animals to
201 transduce the signal, either due to low efficiency of the knockdowns, or to protein
202 stability; (2) the IRFs may act redundantly with each other, and therefore no effect will
203 be seen in single knockdown experiments; or (3) nvIRFs and nvSTAT may not play a
204 role in the response to 2'3'-cGAMP.

205 NF- κ B is also known to act downstream of mammalian STING, and appears to
206 be functionally conserved in *N. vectensis* (43). We found that NF- κ B signaling

207 components are transcriptionally induced by 2'3'-cGAMP (Fig. 1A). To test the role of
208 nvNF- κ B in the 2'3'-cGAMP response, we microinjected embryos with shRNAs targeting
209 nvNF- κ B, treated with 2'3'-cGAMP, and performed RNA-Seq (Fig. 2A). 241 genes were
210 transcribed at significantly lower levels in the nvNF- κ B knockdown embryos, and of
211 these, 98 were genes induced by 2'3'-cGAMP. Of these genes, 40 are uncharacterized,
212 and no GO terms were significantly enriched (data not shown). Of the induced genes
213 that were annotated in NCBI, we noticed many were homologs of anti-bacterial proteins,
214 including homologs of perforin-2/Mpeg-1, LPS-binding protein (LBP), linear gramicidin
215 synthase, and mucins. We confirmed that 2'3'-cGAMP-mediated induction of these
216 putative anti-bacterial genes was NF- κ B dependent by performing qRT-PCR and
217 Nanostring (Fig. 2B; Fig. S5A). Of note, the induction of nvLysozyme was not nvNF- κ B
218 dependent (both by RNA-Seq and qRT-PCR; Fig. S5B), indicating either the existence
219 of another pathway for anti-bacterial gene induction, or that our knockdown experiment
220 was not able to affect expression of all nvNF- κ B dependent genes. In addition, all of the
221 putative anti-viral genes we examined appeared to be induced independent of nvNF- κ B
222 (Fig. S5).

223 We performed BLAST searches of unannotated 2'3'-cGAMP-induced, nvNF- κ B-
224 dependent genes and identified several other genes with predicted anti-bacterial
225 activity, including two homologs of bacterial *tae4* genes, and a putative guanylate
226 binding protein (GBP) (*N. vectensis* LOC5515806, hereafter nvGBP-806). The *Tae4*
227 homologs had been previously identified and will be referred to as nvDae4 proteins
228 (discussed further below; (46)). To confirm the identity of nvGBP-806 as a true GBP
229 homolog, we performed phylogenetic analysis. We identified four conserved *N.*
230 *vectensis* proteins harboring an N-terminal GBP GTPase domain with conserved GBP-
231 specific motifs, including nvGBP-806 (Fig. S6). All of the nvGBP homologs cluster with
232 vertebrate IFN-inducible GBPs and are themselves induced by 2'3'-cGAMP. Finally, we
233 identified several unannotated nvNF- κ B dependent, 2'3'-cGAMP-induced genes that
234 appeared to be cnidarian-specific with no identifiable homologs in other animal phyla
235 (Table S1).

236 To test directly whether nvNF- κ B is activated in *N. vectensis* upon 2'3'-cGAMP
237 treatment, we treated polyps with cGAMP and performed immunostaining for nvNF- κ B
238 (Fig. 2C). Inactive NF- κ B is localized to the cytosol, and we observed sparse, cytosolic
239 staining of ectodermal cells in untreated animals, as has been previously reported (43).
240 In contrast, in 2'3'-cGAMP treated animals, we found many more nvNF- κ B-positive
241 cells, and in almost all of these, nvNF- κ B was found in the nucleus. We performed
242 automated quantification of nuclear nvNF- κ B staining, and found that ~3-20% of nuclei
243 captured in our images were positive for nvNF- κ B (Fig. 2D). In sum, 2'3'-cGAMP leads
244 to nvNF- κ B nuclear localization, and nvNF- κ B appears to be required for expression of
245 many putative anti-bacterial, but not anti-viral, genes. Our results demonstrate the first
246 NF- κ B agonist in *N. vectensis*, and indicate a conserved immune function for NF- κ B in
247 this organism.

248 *Gene induction during Pseudomonas aeruginosa challenge*

250 In order to test whether the putative anti-bacterial, NF- κ B-dependent genes may
251 indeed be important for anti-bacterial immunity, we tested whether these genes were
252 induced during bacterial challenge of *N. vectensis*. *Pseudomonas aeruginosa* is a
253 pathogenic Gram-negative bacterium that can infect a range of hosts, including plants,
254 mammals, and hydra (47, 48), though infections of *N. vectensis* have not previously
255 been reported. Infection of *N. vectensis* polyps with the *P. aeruginosa* strain PA14 led to
256 polyp death in a dose and temperature dependent manner (Fig. 3A). 48 hours after

257 infection, we isolated RNA from infected polyps and assayed gene expression.
258 Interestingly, nvSTING expression was induced during PA14 infection (Fig. 3B), and
259 many of the putative anti-bacterial genes we identified as 2'3'-cGAMP-induced were
260 also induced during infection (Fig. 3C). Importantly, PA14 only produces c-di-GMP and
261 not other CDNs. Since c-di-GMP was not sufficient to robustly activate gene expression
262 in *N. vectensis*, we believe that it is likely that the response to PA14 is independent of
263 bacterial CDNs, although we cannot rule out an effect from PA14-produced c-di-GMP.
264 Nevertheless, taken together, these results indicate that the putative anti-bacterial
265 genes we identified as induced by 2'3'-cGAMP are also induced after bacterial
266 challenge.

267

268 *nvDae4 is a peptidoglycan-cleaving enzyme with anti-bacterial activity*

269 We decided to investigate directly whether some of the genes induced by both
270 2'3'-cGAMP and bacterial infection are in fact anti-bacterial. Type VI secretion amidase
271 effector (Tae) proteins are bacterial enzymes that are injected into neighboring cells to
272 cleave peptidoglycan, an essential component of bacterial cell walls, leading to rapid
273 cell death (49). While the *tae* genes originated in bacteria, they have been horizontally
274 acquired multiple times in evolution by eukaryotes, and at least one of these so-called
275 “domesticated amidase effectors” (Daes) also has bactericidal activity (46, 50). The *N.*
276 *vectensis* genome has two *tae4* homologs, both of which were upregulated by 2'3'-
277 cGAMP in an nvNF- κ B-dependent manner. However, only one of the *N. vectensis* Dae
278 proteins is predicted to encode a conserved catalytic cysteine (46) required for
279 peptidoglycan hydrolysis. Therefore, we focused our efforts on this homolog, which we
280 call nvDae4 (GI: 5507694). We first tested whether nvDae4 has conserved bactericidal
281 properties by expressing nvDae4 in *E. coli* either with or without a periplasm-targeting
282 signal sequence and measuring bacterial growth (assessed by OD₆₀₀) over time (Fig.
283 4A). *E. coli* are Gram-negative bacteria and thus have peptidoglycan
284 compartmentalized within the periplasmic space. Consistent with the predicted
285 peptidoglycan-cleaving function of nvDae4, only periplasmic wild-type (WT) but not
286 catalytic mutant (C63A) nvDae4 expression led to bacterial lysis. In order to test directly
287 whether nvDae4 cleaves peptidoglycan, we produced recombinant protein in insect
288 cells. Since nvDae4 encodes a secretion signal, recombinant nvDae4 was secreted by
289 the insect cells and purified from the cell supernatant. Purified nvDae4 protein was
290 incubated with purified peptidoglycan from either *E. coli* or *Staphylococcus epidermis*.
291 Analysis by high performance liquid chromatography (HPLC) showed that nvDae4
292 cleaves both Gram-negative (Fig. 4B) and Gram-positive (Fig. S7) derived
293 peptidoglycan. Finally, we wondered whether nvDae4 could directly kill Gram-positive
294 bacteria, as these bacteria contain a peptidoglycan cell wall that is not protected by an
295 outer membrane and is therefore accessible to extracellular factors. We treated *B.*
296 *subtilis* with recombinant nvDae4 and found that bacteria treated with WT but not C63A
297 nvDae4 protein were killed (Fig. 4C) in a dose-dependent manner (Fig. 4D). Overall
298 these results show that the 2'3'-cGAMP-induced protein nvDae4 is a peptidoglycan-
299 cleaving enzyme with the capacity to kill bacteria.

300

301 *nvLBP disrupts bacterial membranes*

302 We next wondered whether any of the putative anti-bacterial proteins could
303 directly target Gram-negative bacteria. LPS-binding proteins (LBPs) and
304 bactericidal/permeability-increasing proteins (BPIs) are related, evolutionarily ancient
305 proteins involved in binding, permabilizing, and/or killing Gram-negative bacteria (51).
306 *N. vectensis* has two LBP/BPI homologs, and we focused our efforts on one (GI:

307 5508577; called nvLBP due to its isoelectric point being more similar to that of human
308 LBP), which we found to be induced by both *P. aeruginosa* infection, and by 2'3'-
309 cGAMP in an nvNF- κ B-dependent manner (Fig. 1A, 1C, 2A, 2B, 3C). We purified
310 recombinant nvLBP protein from insect cell supernatants and incubated it with *P.*
311 *aeruginosa* or *E. coli*, but never saw an impact on bacterial survival (data not shown).
312 We then hypothesized that nvLBP could instead permeabilize outer membranes, which
313 alone might not lead to bacterial lysis, but which might synergize with other anti-
314 bacterial factors during an immune responses (52). To test for membrane
315 permeabilization, we performed 1-*N*-phenyl-naphthylamine (NPN) uptake assays with *P.*
316 *aeruginosa*. NPN fluoresces weakly in aqueous solution but strongly in the presence of
317 phospholipids, which are exposed in Gram-negative bacteria when the outer membrane
318 is disrupted (53). Indeed, in the absence of nvLBP or gentamicin, very little fluorescence
319 was detected; however, upon addition of gentamicin, an antibiotic known to disrupt the
320 Gram-negative outer membrane, or upon addition of nvLBP, we detected a significant
321 increase in fluorescence, indicating that nvLBP does indeed permeabilize *P. aeruginosa*
322 membranes (Figure 4E). Thus, upon 2'3'-cGAMP sensing or *P. aeruginosa* infection, *N.*
323 *vectensis* produces proteins capable of targeting both Gram-positive and Gram-
324 negative bacteria.

325 326 Discussion

327 In this study, we identified hundreds of *N. vectensis* genes that are induced by
328 the STING ligand 2'3'-cGAMP. Despite over 600 million years of divergence and the
329 absence of interferons, *N. vectensis* responds to 2'3'-cGAMP similarly to mammals by
330 inducing a variety of anti-viral genes. Similarly, Lewandowska et al. (45) reported that *N.*
331 *vectensis* responds to the synthetic double-stranded RNA poly(I:C), a viral mimic and
332 pathogen-associated molecular pattern (PAMP). In *N. vectensis*, poly(I:C) induced both
333 RNAi pathway components and genes traditionally thought of as vertebrate ISGs. Our
334 combined findings indicate that the pathways linking PAMP detection to ISG expression
335 existed prior to the vertebrate innovation of type I IFNs. Interestingly, some invertebrate
336 species have protein-based anti-viral signaling pathways that perform similar functions
337 to type I IFNs in vertebrates. For example, mosquito cells secrete the peptide Vago
338 upon viral infection, which signals through the JAK-STAT pathway to activate anti-viral
339 immunity (54). Additionally, the oyster *Crassostrea gigas* is thought to have an IFN-like
340 system, but no secreted proteins have yet been identified in this organism (55). *N.*
341 *vectensis* may also encode an undiscovered IFN-like protein; at a minimum, *N.*
342 *vectensis* encodes several IRF-like genes (Fig. S3). One attractive hypothesis is that
343 these IRFs are important for the anti-viral response of *N. vectensis*; however, we were
344 unable to see any impact of single knockdown experiments on the induction of genes by
345 2'3'-cGAMP, though this may be explained by redundancy or technical limitations of our
346 knockdown approach. Nevertheless, an important conclusion of our work is that
347 induction of a broad transcriptional program is an ancestral function of 2'3'-cGAMP
348 signaling, similar to what has been seen in *Drosophila* (31) and choanoflagellates (56).
349 This ancestral transcriptional response complements an additional autophagy response
350 to 2'3'-cGAMP that was previously reported to be induced by nvSTING in mammalian
351 cells (17), and has now also been shown to be induced by 2'3'-cGAMP and STING in
352 choanoflagellates (56).

353 We found that in addition to an anti-viral response, *N. vectensis* responds to 2'3'-
354 cGAMP by inducing a variety of anti-bacterial genes, including lysozyme, Dae4,
355 perforin-2-like, LPB, and GBPs. With the exception of GBPs, which have dual anti-viral
356 and anti-bacterial activity, these anti-bacterial genes are not induced by 2'3'-cGAMP in

357 vertebrates; thus, the anti-bacterial response appears to be a unique feature of 2'3'-
358 cGAMP signaling in *N. vectensis*, and it will be interesting to see whether this proves
359 true in other invertebrates, or in additional cell types or contexts in vertebrates. Several
360 of the anti-bacterial genes are also induced by poly(I:C) (45), perhaps indicating a
361 broader anti-pathogen response to PAMPs in *N. vectensis*. Interestingly, we found that
362 nvNF- κ B was specifically required for the induction of many of these anti-bacterial
363 genes. This suggests that nvNF- κ B activation downstream of 2'3'-cGAMP signaling may
364 have been present in the most recent common ancestor of cnidarian and mammals, and
365 confirms a role for nvNF- κ B in *N. vectensis* immunity. Consistent with this speculation,
366 *Drosophila* STING also appears to activate NF- κ B (30, 31, 34).

367 To further establish that 2'3'-cGAMP induces proteins with anti-bacterial activity, we
368 functionally characterized two 2'3'-cGAMP-induced, nvNF- κ B-dependent proteins,
369 nvDae4 and nvLBP. We found that nvDae4 is a peptidoglycan-cleaving enzyme with
370 direct bactericidal activity against Gram-positive bacteria. In addition, we found that
371 nvLBP permeabilizes Gram-negative bacterial membranes. Many of the 2'3'-cGAMP-
372 induced NF- κ B dependent genes are not recognizable homologs of proteins of known
373 function; thus, they represent good candidates for the discovery of novel anti-bacterial
374 genes in *N. vectensis*.

375 Using shRNAs to knockdown nvSTING failed to confirm an essential role for
376 nvSTING in the response to 2'3'-cGAMP. However, our previous biochemical and
377 structural studies showed nvSTING binds 2'3'-cGAMP with high affinity ($K_d < 1$ nM) and
378 in a very similar manner as vertebrate STING (37). STING is essential for the response
379 to 2'3'-cGAMP in diverse organisms, including vertebrates, choanoflagellates (56), and
380 insects (31). In addition, nvSTING is highly induced by 2'3'-cGAMP. So despite our
381 negative results, we favor the idea that nvSTING is at least partially responsible for the
382 response of *N. vectensis* to 2'3'-cGAMP. It is possible that *N. vectensis* encodes a
383 redundant 2'3'-cGAMP sensor, but such a sensor would have had to evolve specifically
384 in Cnidarians, or lost independently from choanoflagellates, insects and vertebrates. It is
385 likely that technical limitations of performing shRNA knockdowns in *N. vectensis*
386 accounts for our inability to observe a role for nvSTING in the response to 2'3'-cGAMP,
387 though we cannot exclude the possibility that *N. vectensis* utilizes a distinct 2'3'-
388 cGAMP-sensing pathway.

389 If indeed 2'3'-cGAMP is signaling via nvSTING, this presents several mechanistic
390 questions. First, in mammals, all known signaling downstream of STING, including NF-
391 κ B activation, requires the CTT (38), leading to the question of how invertebrate STING
392 proteins, which lack a discrete CTT, can activate this pathway. Also, nvNF- κ B
393 knockdown did not impact the vast majority of 2'3'-cGAMP-induced genes, which may
394 imply the existence of other signaling pathways downstream of nvSTING. How these
395 unidentified pathways become activated is another interesting question and one that
396 could also shed light on mammalian STING signaling. Finally, mammalian STING can
397 also be activated by direct binding to bacterial 3'3'-linked CDNs (57), and nvSTING also
398 binds to these ligands, albeit with lower affinity (37). We found that treatment of *N.*
399 *vectensis* with these ligands also led to induction of many of the same genes, likely
400 through the same pathway. This perhaps indicates a role for the nvSTING pathway in
401 bacterial sensing, though our preliminary attempts to observe an impact of 2'3'-cGAMP-
402 induced gene expression on bacterial colonization of *N. vectensis* were unsuccessful.
403 Further development of a bacterial infection model for *N. vectensis* will be required to
404 study the anti-bacterial response of this organism *in vivo*.

405 A crucial remaining question is what activates nvcGAS to produce 2'3'-cGAMP.
406 Double-stranded DNA did not seem to activate this protein *in vitro* (37), but this could be

407 due to the absence of cofactors. This protein is also constitutively active when
408 transfected into mammalian cells, but this could be due to overexpression.
409 Unlike human cGAS, nvcGAS does not have any clear DNA-binding domains, although
410 this does not necessarily exclude DNA as a possible ligand. The *Vibrio* cGAS-like
411 enzyme DncV is regulated by folate-like molecules (58), so there is a diverse range of
412 possible nvcGAS activators. Understanding the role of the cGAS-cGAMP-STING
413 pathway in diverse organisms can shed light on the mechanisms of evolution of viral
414 and bacterial sensing, and on unique ways divergent organisms have evolved to
415 respond to pathogens.

416

417 **Methods**

418

419 ***Nematostella vectensis* culture and spawning**

420 *N. vectensis* adults were a gift from Mark Q. Martindale (University of Florida)
421 and were cultured and spawned as previously described (59). Briefly, animals were kept
422 in 1/3x seawater (12ppt salinity) in the dark at 17°C and fed freshly hatched *Artemia*
423 (Carolina Biological Supply Company) weekly. Spawning was induced every two weeks
424 by placing animals at 23°C under bright light for 8 hours, followed by 2 hours in the
425 dark, and then finally moved to the light where they were monitored for spawning. Egg
426 masses were de-jellied in 4% L-Cysteine (pH 7-7.4) in 1/3x sea water for 10-15 minutes
427 and washed 3 times with 1/3x sea water. Water containing sperm was added to the
428 washed eggs and these were either used immediately for microinjection or allowed to
429 develop at room temperature.

430

431 **CDN treatment**

432 For the RNA sequencing experiment on polyps (Fig. 1 and Fig. S1), ~4 week old
433 polyps were treated in duplicate in a bath of 500µM c-di-AMP, c-di-GMP, 2'3'-cGAMP,
434 or 3'3'-cGAMP (all InvivoGen) in 1/3x sea water for 24 hours. For remaining cGAMP
435 treatment experiments, 50-100 48-hour old embryos were treated with 100µM 2'3'-
436 cGAMP (InvivoGen) in 1/3x sea water for 4 hours.

437

438 **RNA sequencing**

439 For the initial CDN treatment experiment using polyps, total RNA was extracted
440 using Qiagen RNeasy Mini kits according to the manufacturer's protocol. Libraries were
441 prepared by the Functional Genomics Laboratory at UC Berkeley using WaferGen
442 PrepX library prep kits with oligo dT beads for mRNA enrichment according to the
443 manufacturer's protocol, and 50 nt single-end sequencing was carried out on the
444 HiSeq4000 (Illumina) by the Vincent J.Coates Genomics Sequencing Laboratory. For all
445 other RNA sequencing experiments on 48 hour embryos, RNA was extracted using
446 Trizol (Thermo Fisher Scientific) according to the manufacturer's protocol. Libraries
447 were prepared by the Functional Genomics Laboratory at UC Berkeley as follows: oligo
448 dT beads from the KAPA mRNA Capture Kit (KK8581) were used for mRNA
449 enrichment; fragmentation, adapter ligation and cDNA synthesis were performed using
450 the KAPA RNA HyperPrep kit (KK8540). Libraries were pooled evenly by molarity and
451 sequenced by the Vincent J.Coates Genomics Sequencing Laboratory on a
452 NovaSeq6000 150PE S4 flowcell (Illumina), generating 25M read pairs per sample.
453 Read quality was assessed using FastQC. Reads were mapped to the *N. vectensis*
454 transcriptome (NCBI: GCF_000209225.1) using kallisto and differential expression was
455 analyzed in R with DESeq2. Differential expression was deemed significant with a log₂
456 fold change greater than 1 and an adjusted p-value less than 0.05. GO term analysis

457 was performed using goseq with GO annotations from
458 [https://figshare.com/articles/dataset/Nematostella_vectensis_transcriptome_and_gene](https://figshare.com/articles/dataset/Nematostella_vectensis_transcriptome_and_gene_models_v2_0/807696)
459 [models_v2_0/807696](https://figshare.com/articles/dataset/Nematostella_vectensis_transcriptome_and_gene_models_v2_0/807696). The EnhancedVolcano package
460 (<https://github.com/kevinblighe/EnhancedVolcano>) was used to generate volcano plots.
461 Heatmaps are based on regularized log-transformed normalized counts and Z-scores
462 are scaled by row. All RNA-Seq results can be found in Supplementary File S1.

463 **Quantitative Real-Time PCR (qRT-PCR)**

464 Embryos and polyps were lysed in TRIzol (Invitrogen) and RNA was extracted
465 according to the manufacturer's protocol. 500ng of RNA was treated with RQ1 RNase-
466 free DNase (Promega) for and reverse transcribed with Superscript III (Invitrogen).
467 Quantitative PCR was performed using SYBR Green (Thermo Fisher Scientific) with 0.8
468 μM of forward and reverse primers on a QuantStudio 5 Real-Time PCR System
469 (Applied Biosystems) with the following cycling conditions: 50°C 2 min; 95°C 10 min;
470 [95°C 15 sec, 60°C 1 min] x 40; 95°C 15 sec; 60°C 1 min; melt curve: step 0.075 °C/s to
471 95°C. Fold changes in expression levels were normalized to actin and calculated using
472 the $2^{-\Delta\Delta\text{Ct}}$ method. Student's t-tests were performed on ΔCt values. All primer sequences
473 used in this study can be found in Supplementary File S2.

474 **shRNA microinjection**

475 Short hairpin RNAs for microinjection were prepared by *in vitro* transcription as
476 previously described (60). Briefly, unique 19 nucleotide targeting motifs were identified
477 and used to create oligonucleotides with the following sequence: T7 promoter—19nt
478 motif—linker—antisense 19nt motif—TT. RNA secondary structure was visualized using
479 mfold (<http://www.unafold.org/mfold/applications/rna-folding-form.php>) to ensure a
480 single RNA conformation. Both sense and anti-sense oligonucleotides were synthesized
481 and mixed to a final concentration of 25 μM , heated to 98°C for 5 minutes and cooled to
482 24°C before use as template for *in vitro* transcription using the Ampliscribe T7-Flash
483 Transcription Kit (Lucigen). Reactions were allowed to proceed overnight, followed by a
484 15 minute treatment with DNase and subsequent purification with Direct-zol™ RNA
485 MiniPrep Plus (Zymo Research). All shRNAs used in this study can be found in
486 Supplementary File S2.

487 Microinjections of one-cell embryos were carried out as previously described
488 (61). shRNAs were diluted to a concentration of 500-900 ng/ μl (ideal concentrations
489 were determined experimentally) in RNase-free water with fluorescent dextran for
490 visualization. Injected embryos were monitored for gross normal development at room
491 temperature and used for experiments 48 hours later unless otherwise indicated.
492 Knockdowns for each gene were performed using at least two different shRNAs and
493 phenotypes were confirmed in at least 3 independent experiments.

494 **Immunohistochemistry, imaging, and quantification**

495 Polyps treated for 4 hours with 100 μM 2'3'-cGAMP were stained for nvNF- κB as
496 previously described (62). Briefly, polyps were fixed in 4% paraformaldehyde in 1/3x
497 sea water overnight at 4°C with rocking, and subsequently washed 3 times with wash
498 buffer (1x PBS, 0.2% Triton X-100). Antigen retrieval was performed by placing
499 anemones in 95°C 5% urea for 5 minutes and allowing them to cool to room
500 temperature before washing 3 times in wash buffer. Samples were blocked overnight at
501 4°C in blocking buffer (1x PBS, 5% normal goat serum, 1% bovine serum albumin,
502 0.2% Triton X-100). Samples were stained with anti-nvNF- κB (1:100; gift of Thomas
503 Gilmore, Boston University) in blocking buffer for 90 minutes at room temperature and
504

507 washed 4 times in wash buffer. Samples were then incubated in FITC-anti-Rabbit IgG
508 (1:160; F9887, Sigma-Aldrich) in blocking buffer for 90 minutes at 37°C. Finally,
509 samples were washed in wash buffer, stained with 1 µg/mL of DAPI for 10 minutes,
510 washed again, and mounted in Vectashield HardSet Mounting medium and imaged on a
511 Zeiss LSM 710 AxioObserver. Imaris 9.2 (Bitplane) was used to create 3D surfaces
512 based on DAPI expression, and surface statistics were exported and analyzed in
513 FlowJo (BD) to quantify nuclear nvNF-κB expression as previously described (63).

514

515 **Bacterial infection**

516 Single colonies of *Pseudomonas aeruginosa* strain PA14-GFP were cultured
517 overnight in LB with 50 µg/ml of carbenicillin, centrifuged for 5 minutes at 3000 x g,
518 resuspended to an OD₆₀₀ of 0.1, 0.01, or 0.001 in 1/3x sea water and used to infect
519 polyps, which were kept at room temperature or 28°C as indicated. Inputs were plated
520 to calculate CFU/ml. Polyp survival was monitored daily. For expression analysis,
521 polyps were homogenized in Trizol and RNA extraction and qPCR were performed as
522 indicated above.

523

524 **Protein purification**

525 Double-stranded DNA encoding codon optimized nvLBP lacking its signal
526 peptide was ordered from IDT, and nvDae4 lacking its signal peptide was cloned from
527 cDNA. These fragments were then cloned into the pAcGP67-A baculovirus transfer
528 vector for secreted, His-tagged protein expression. The plasmid for expressing mutant
529 nvDae4 (C63A) was made from the pAcGP67-A-nvDae4 plasmid using Q5 site-directed
530 mutagenesis (NEB) according to the manufactures protocol. Plasmids were transfected
531 into Sf9 insect cells (2x10⁶ cells/ml in 2ml) using Cellfectin II Reagent (Gibco) along with
532 BestBac 2.0 v-cath/chiA Deleted Linearized Baculovirus DNA (Expression Systems) for
533 6 hours, after which media was replaced and cells were left for 1 week at 25°C.
534 Supernatants were harvested and 50 µL were used to infect 7x10⁶ Sf9 cells in 10ml of
535 media for 1 week at 25°C. Supernatants containing secondary virus were harvested,
536 tested, and used to infect High Five cells (2 L at 1.5x10⁶ cells/ml) for 72 hours at 25°C
537 with shaking. Supernatants containing protein were harvested by centrifuging for 15 min
538 at 600 x g at 4°C and subsequently passing through a 0.45 µm filter to remove all cells.
539 Supernatants were buffered to 1x HBS (20mM HEPES pH 7.2, 150mM NaCl), mixed
540 with 2 mL of Ni-NTA agarose were per liter, and rotated at 4°C for 2 hours. Ni-NTA
541 resins with bound protein were collected on a column by gravity-flow and washed with
542 30x column volume of wash buffer (for nvDae4: 20mM HEPES, 1M NaCl, 30mM
543 imidazole, 10% glycerol; for nvLBP: 20mM HEPES, 400mM NaCl, 20mM imidazole).
544 Protein was eluted in 1 mL fractions using 1xHBS supplemented with 200mM imidazole.
545 Buffer was exchanged to 1xHBS+ 2mM DTT using Econo-Pac10DG Desalting
546 Prepacked Gravity Flow Columns (Bio-rad) according to the manufacturers protocol,
547 and proteins were concentrated using 10kDa (for nvDae4) or 30kDa (for nvLBP)
548 concentrators (Millipore).

549

550 **Bacterial killing assays**

551 For expression in *E. coli*, nvDae4 WT and C63A lacking the endogenous signal
552 sequence were cloned into the pET28a vector for inducible cytosolic expression, or the
553 pET22b vector for inducible periplasmic expression. *E. coli* (BL21 DE3 strain) were
554 freshly transformed with the vectors and grown overnight in LB with 50 µg/mL
555 carbenicillin shaking at 37°C. Overnight cultures were backdiluted in LB to the same

556 OD₆₀₀ and grown to log phase before induction with 0.25mM IPTG. Plates were kept
557 shaking at 37°C and OD₆₀₀ was read every 5 minutes for 3 hours.

558 *Bacillus subtilis*-GFP (derivative of strain 168; BGSC accession #1A1139) was
559 grown to log-phase in LB with 100 µg/mL spectinomycin, centrifuged, resuspended in
560 0.5xHBS, and incubated alone or with nvDae4 WT or C63A at indicated concentrations
561 for 2-3 hours at 37°C. Serial dilutions were plated on LB agar with 100 µg/mL
562 spectinomycin to determine CFU.

563

564 **Peptidoglycan cleavage assays**

565 Peptidoglycan (PG) was purified and analyzed as previously described (50).
566 Briefly, *Escherichia coli* BW11325 (from Carol Gross, UCSF) and *Staphylococcus*
567 *epidermis* BCM060 (from Tiffany Scharschmidt, UCSF) were grown to an OD₆₀₀ of 0.6,
568 harvested by centrifugation, and boiled in SDS (4 % final concentration) for 4 hours with
569 stirring. After washing in purified water to remove SDS, the peptidoglycan was treated
570 with Pronase E for 2 h at 60°C (0.1 mg/ml final concentration in 10 mM Tris-HCl pH7.2
571 and 0.06 % NaCl; pre-activated for 2 h at 60 °C). Pronase E was heat inactivated at
572 100°C for 10 min and washed with sterile filtered water (5 x 20 min at 21k × g). PG from
573 Gram-positive bacteria (Se) was also treated with 48% HF at 37°C for 48 h to remove
574 teichoic acids, followed by washes with sterile filtered water. nvDae4 enzyme (WT and
575 C63A) was added (1-10 µM in 10 mM Tris-HCl pH 7.2 and 0.06% NaCl) and incubated
576 O/N at 37°C. Enzymes were heat inactivated at 100°C for 10 min. Mutanolysin (Sigma
577 M9901, final concentration 20 µg/ml) was added to the purified peptidoglycan and
578 incubated overnight at 37 °C. The peptidoglycan fragments were reduced, acidified,
579 analyzed via HPLC (0.5 ml/min flow rate, 55°C with Hypersil ODS C18 HPLC column,
580 Thermo Scientific, catalog number: 30103-254630).

581

582 **NPN uptake assay**

583 PA14-GFP cultures were grown from a single colony for 8 hours shaking at 37°C,
584 then 500µL were used to inoculate a 50 mL culture overnight. 25 mL of culture were
585 centrifuged at 600 x g for 10 minutes and resuspended in 1 M HEPES to an OD₆₀₀ of
586 0.2-0.4. 96 µL of PA14 culture were added to the wells of a blacked-walled 96-well plate
587 along with 2 µL of 500 µM *N*-Phenyl-1-naphthylamine (NPN; Sigma-Aldrich) in acetone
588 or acetone alone. Baseline fluorescence was read every 30 seconds on a Spark
589 microplate reader (Tecan) with the following conditions: 350nm excitation; 420nm
590 emission; manual gain 70%. After 10 minutes, 2 µL of buffer, gentamycin (final
591 concentration 20 µg/mL), or LBP (final concentration 4.6 µM) were added to triplicate
592 wells and fluorescence was read for 20 minutes. Values were normalized to relevant
593 reaction wells without NPN and plotted.

594

595 **Supplemental methods**

596

597 **Phylogenetic analysis**

598 Protein sequences containing domains of interest were downloaded from NCBI,
599 with the exception of nvGBP6 and nvGBP7, for which RNA-seq data showed additional
600 nucleotide usage relative to the reference sequence (all sequences can be found in
601 Supplementary File S2). These were aligned using on phylogeny.fr using MUSCLE and
602 manipulated in Geneious. For the GBP and IRF alignments, only the domain of interest
603 was used for phylogenetic analysis. Maximum likelihood phylogenetic trees were
604 generated with PhyML using 100 bootstrap replicates. Alignments shown were made in
605 Geneious using Clustal Omega.

606
607
608
609
610
611
612
613
614
615
616
617
618
619
620
621
622
623
624
625
626
627
628
629
630
631
632
633
634
635
636
637
638
639
640
641
642
643
644
645
646
647
648
649
650
651
652

Nanostring gene expression analysis

A custom codeset targeting 36 genes of interest and 4 housekeeping genes for normalization (Supplementary File S2) was designed by NanoString Technologies (Seattle, WA) for use in nCounter XT CodeSet Gene Expression Assays run on an nCounter SPRINT Profiler (NanoString Technologies). RNA was isolated as it was for qRT-PCR experiments, and hybridized to probes according to the manufacturer's protocol using 50ng/ μ L of total RNA. Quality control, data normalization, and visualization was performed in nSolver 4.0 analysis software (NanoString Technologies) according to the manufacturer's protocol.

Mammalian cell immunofluorescence and confocal microscopy

Glass coverslips were seeded with 293T cells and grown to ~50% confluency. Cells were transfected for 24-48 hours with a total of 1.25 μ g of DNA and 3 μ L Lipofectamine 2000. Each well contained the following: pcDNA4-STING (10 ng), pEGFP-LC3 (5 ng) and either empty vector or pcDNA4 with the indicated cyclic-dinucleotide synthase (1,235 ng). Cells were washed once in PBS, fixed for 15 minutes in 4% paraformaldehyde, washed once in PBS, and permeabilized for 5 minutes in 0.5% saponin in PBS. Cells were then washed once in PBS, and treated with 0.1% sodium borohydride/0.1% saponin/PBS for 5 – 10 minutes in order to consume any remaining paraformaldehyde. Cells were then washed 3 times in PBS, and blocked with blocking buffer (1% BSA/0.1% saponin/PBS) for 45 minutes. Cells were then incubated HA antibody (1:200 dilution, Sigma 11867423001 rat IgG from Roche) in blocking buffer for one hour and washed 3 times in PBS. Each well was then incubated with 0.1% saponin/PBS and secondary antibody (1:500 dilution, Jackson ImmunoResearch, Cy3 affipure donkey anti-rat IgG, 712-165-153) for 45 minutes. Finally, cells were washed 3 times in PBS, mounted using VectaShield with DAPI, and dried overnight. Images were acquired using a Zeiss LSM 780 NLO AxioExaminer.

Acknowledgements

We are especially grateful to Mark Q. Martindale and Miguel Salinas-Saavedra for *N. vectensis* animals and training. We also thank Matt Gibson for sharing shRNA protocols, and Thomas Gilmore for the anti-nvNF- κ B antibody. We thank members of the Vance and Barton labs for discussions, and Arielle Woznica for comments on the manuscript. This work used the Functional Genomic Laboratory and Vincent J. Coates Genomics Sequencing Laboratory at UC Berkeley, supported by NIH S10 OD018174 Instrumentation Grant. Confocal imaging experiments were conducted at the CRL Molecular Imaging Center supported by the Gordon and Betty Moore Foundation; we would like to thank Holly Aaron and Feather Ives for training and assistance. REV is an HHMI Investigator and is supported by NIH grants AI0663302, AI075039, and AI155634. SRM is supported by the National Science Foundation Graduate Research Fellowship under Grant Numbers DGE 1106400 and DGE 1752814. B.H. and S.C. were supported by funding from the NIH (R01AI132851 to S.C.), the Chan Zuckerberg Biohub, and the Sangvhi-Agarwal Innovation Award. Any opinions, findings, and conclusions or recommendations expressed in this material are those of the author(s) and do not necessarily reflect the views of the National Science Foundation, HHMI, or the National Institutes of Health.

653 References

- 654
- 655 1. J. Ahn, G. N. Barber, STING signaling and host defense against microbial
656 infection. *Exp Mol Med* **51**, 1-10 (2019).
 - 657 2. A. Ablasser, Z. J. Chen, cGAS in action: Expanding roles in immunity and
658 inflammation. *Science* **363** (2019).
 - 659 3. L. Sun, J. Wu, F. Du, X. Chen, Z. J. Chen, Cyclic GMP-AMP synthase is a
660 cytosolic DNA sensor that activates the type I interferon pathway. *Science* **339**,
661 786-791 (2013).
 - 662 4. P. Gao *et al.*, Cyclic [G(2',5')pA(3',5')p] is the metazoan second messenger
663 produced by DNA-activated cyclic GMP-AMP synthase. *Cell* **153**, 1094-1107
664 (2013).
 - 665 5. A. Ablasser *et al.*, cGAS produces a 2'-5'-linked cyclic dinucleotide second
666 messenger that activates STING. *Nature* **498**, 380-384 (2013).
 - 667 6. E. J. Diner *et al.*, The innate immune DNA sensor cGAS produces a
668 noncanonical cyclic dinucleotide that activates human STING. *Cell reports* **3**,
669 1355-1361 (2013).
 - 670 7. X. Zhang *et al.*, Cyclic GMP-AMP containing mixed phosphodiester linkages is
671 an endogenous high-affinity ligand for STING. *Molecular cell* **51**, 226-235 (2013).
 - 672 8. H. Ishikawa, G. N. Barber, STING is an endoplasmic reticulum adaptor that
673 facilitates innate immune signalling. *Nature* **455**, 674-678 (2008).
 - 674 9. Y. Tanaka, Z. J. Chen, STING specifies IRF3 phosphorylation by TBK1 in the
675 cytosolic DNA signaling pathway. *Science signaling* **5**, ra20 (2012).
 - 676 10. S. Liu *et al.*, Phosphorylation of innate immune adaptor proteins MAVS, STING,
677 and TRIF induces IRF3 activation. *Science* **347**, aaa2630 (2015).
 - 678 11. C. Zhang *et al.*, Structural basis of STING binding with and phosphorylation by
679 TBK1. *Nature* **567**, 394-398 (2019).
 - 680 12. B. Zhao *et al.*, A conserved PLPLRT/SD motif of STING mediates the recruitment
681 and activation of TBK1. *Nature* **569**, 718-722 (2019).
 - 682 13. D. B. Stetson, R. Medzhitov, Type I interferons in host defense. *Immunity* **25**,
683 373-381 (2006).
 - 684 14. J. W. Schoggins, Interferon-Stimulated Genes: What Do They All Do? *Annu Rev*
685 *Virol* **6**, 567-584 (2019).
 - 686 15. T. Abe, G. N. Barber, Cytosolic-DNA-mediated, STING-dependent
687 proinflammatory gene induction necessitates canonical NF-kappaB activation
688 through TBK1. *Journal of virology* **88**, 5328-5341 (2014).
 - 689 16. H. Chen *et al.*, Activation of STAT6 by STING is critical for antiviral innate
690 immunity. *Cell* **147**, 436-446 (2011).
 - 691 17. X. Gui *et al.*, Autophagy induction via STING trafficking is a primordial function of
692 the cGAS pathway. *Nature* **567**, 262-266 (2019).
 - 693 18. T. D. Fischer, C. Wang, B. S. Padman, M. Lazarou, R. J. Youle, STING induces
694 LC3B lipidation onto single-membrane vesicles via the V-ATPase and ATG16L1-
695 WD40 domain. *J Cell Biol* **219** (2020).
 - 696 19. R. O. Watson, P. S. Manzanillo, J. S. Cox, Extracellular *M. tuberculosis* DNA
697 targets bacteria for autophagy by activating the host DNA-sensing pathway. *Cell*
698 **150**, 803-815 (2012).

- 699 20. R. O. Watson *et al.*, The Cytosolic Sensor cGAS Detects Mycobacterium
700 tuberculosis DNA to Induce Type I Interferons and Activate Autophagy. *Cell host*
701 *& microbe* **17**, 811-819 (2015).
- 702 21. S. Gluck, A. Ablasser, Innate immunosensing of DNA in cellular senescence.
703 *Current opinion in immunology* **56**, 31-36 (2019).
- 704 22. M. M. Gaidt *et al.*, The DNA Inflammasome in Human Myeloid Cells Is Initiated
705 by a STING-Cell Death Program Upstream of NLRP3. *Cell* **171**, 1110-1124
706 e1118 (2017).
- 707 23. A. Sze *et al.*, Host restriction factor SAMHD1 limits human T cell leukemia virus
708 type 1 infection of monocytes via STING-mediated apoptosis. *Cell host &*
709 *microbe* **14**, 422-434 (2013).
- 710 24. S. R. Paludan, L. S. Reinert, V. Hornung, DNA-stimulated cell death: implications
711 for host defence, inflammatory diseases and cancer. *Nature reviews.*
712 *Immunology* **19**, 141-153 (2019).
- 713 25. M. F. Gulen *et al.*, Signalling strength determines proapoptotic functions of
714 STING. *Nature communications* **8**, 427 (2017).
- 715 26. J. Wu *et al.*, STING-mediated disruption of calcium homeostasis chronically
716 activates ER stress and primes T cell death. *The Journal of experimental*
717 *medicine* **216**, 867-883 (2019).
- 718 27. S. R. Margolis, S. C. Wilson, R. E. Vance, Evolutionary Origins of cGAS-STING
719 Signaling. *Trends Immunol* **38**, 733-743 (2017).
- 720 28. D. Cohen *et al.*, Cyclic GMP-AMP signalling protects bacteria against viral
721 infection. *Nature* **574**, 691-695 (2019).
- 722 29. B. R. Morehouse *et al.*, STING cyclic dinucleotide sensing originated in bacteria.
723 *Nature* **586**, 429-433 (2020).
- 724 30. A. Goto *et al.*, The Kinase IKKbeta Regulates a STING- and NF-kappaB-
725 Dependent Antiviral Response Pathway in Drosophila. *Immunity* **49**, 225-234
726 e224 (2018).
- 727 31. H. Cai *et al.*, 2'3'-cGAMP triggers a STING- and NF-kappaB-dependent broad
728 antiviral response in Drosophila. *Science signaling* **13** (2020).
- 729 32. Y. Liu *et al.*, Inflammation-Induced, STING-Dependent Autophagy Restricts Zika
730 Virus Infection in the Drosophila Brain. *Cell host & microbe* **24**, 57-68 e53 (2018).
- 731 33. X. Hua *et al.*, Stimulator of interferon genes (STING) provides insect antiviral
732 immunity by promoting Dredd caspase-mediated NF-kappaB activation. *J Biol*
733 *Chem* **293**, 11878-11890 (2018).
- 734 34. M. Martin, A. Hiroyasu, R. M. Guzman, S. A. Roberts, A. G. Goodman, Analysis
735 of Drosophila STING Reveals an Evolutionarily Conserved Antimicrobial
736 Function. *Cell reports* **23**, 3537-3550 e3536 (2018).
- 737 35. X. Hua, W. Xu, S. Ma, Q. Xia, STING-dependent autophagy suppresses Nosema
738 bombycis infection in silkworms, Bombyx mori. *Developmental and comparative*
739 *immunology* **115**, 103862 (2021).
- 740 36. N. H. Putnam *et al.*, Sea anemone genome reveals ancestral eumetazoan gene
741 repertoire and genomic organization. *Science* **317**, 86-94 (2007).
- 742 37. P. J. Kranzusch *et al.*, Ancient Origin of cGAS-STING Reveals Mechanism of
743 Universal 2',3' cGAMP Signaling. *Molecular cell* **59**, 891-903 (2015).
- 744 38. L. H. Yamashiro *et al.*, Interferon-independent STING signaling promotes
745 resistance to HSV-1 in vivo. *Nature communications* **11**, 3382 (2020).

- 746 39. S. Yum, M. Li, Y. Fang, Z. J. Chen, TBK1 recruitment to STING activates both
747 IRF3 and NF-kappaB that mediate immune defense against tumors and viral
748 infections. *Proceedings of the National Academy of Sciences of the United*
749 *States of America* **118** (2021).
- 750 40. D. J. Miller *et al.*, The innate immune repertoire in cnidaria--ancestral complexity
751 and stochastic gene loss. *Genome Biol* **8**, R59 (2007).
- 752 41. A. M. Reitzel, J. C. Sullivan, N. Traylor-Knowles, J. R. Finnerty, Genomic survey
753 of candidate stress-response genes in the estuarine anemone *Nematostella*
754 *vectensis*. *Biol Bull* **214**, 233-254 (2008).
- 755 42. J. J. Brennan *et al.*, Sea anemone model has a single Toll-like receptor that can
756 function in pathogen detection, NF-kappaB signal transduction, and
757 development. *Proceedings of the National Academy of Sciences of the United*
758 *States of America* **114**, E10122-E10131 (2017).
- 759 43. F. S. Wolenski *et al.*, Characterization of the core elements of the NF-kappaB
760 signaling pathway of the sea anemone *Nematostella vectensis*. *Molecular and*
761 *cellular biology* **31**, 1076-1087 (2011).
- 762 44. F. S. Wolenski, C. A. Bradham, J. R. Finnerty, T. D. Gilmore, NF-kappaB is
763 required for cnidocyte development in the sea anemone *Nematostella vectensis*.
764 *Developmental biology* **373**, 205-215 (2013).
- 765 45. M. Lewandowska, T. Sharoni, Y. Admoni, R. Aharoni, Y. Moran, Functional
766 characterization of the cnidarian antiviral immune response reveals ancestral
767 complexity. *bioRxiv* 10.1101/2020.11.12.379735, 2020.2011.2012.379735
768 (2020).
- 769 46. S. Chou *et al.*, Transferred interbacterial antagonism genes augment eukaryotic
770 innate immune function. *Nature* **518**, 98-101 (2015).
- 771 47. L. G. Rahme *et al.*, Plants and animals share functionally common bacterial
772 virulence factors. *Proceedings of the National Academy of Sciences of the United*
773 *States of America* **97**, 8815-8821 (2000).
- 774 48. S. Franzenburg *et al.*, MyD88-deficient Hydra reveal an ancient function of TLR
775 signaling in sensing bacterial colonizers. *Proceedings of the National Academy of*
776 *Sciences of the United States of America* **109**, 19374-19379 (2012).
- 777 49. A. B. Russell *et al.*, Type VI secretion delivers bacteriolytic effectors to target
778 cells. *Nature* **475**, 343-347 (2011).
- 779 50. B. M. Hayes *et al.*, Ticks Resist Skin Commensals with Immune Factor of
780 Bacterial Origin. *Cell* **183**, 1562-1571 e1512 (2020).
- 781 51. B. C. Krasity, J. V. Troll, J. P. Weiss, M. J. McFall-Ngai, LBP/BPI proteins and
782 their relatives: conservation over evolution and roles in mutualism. *Biochem Soc*
783 *Trans* **39**, 1039-1044 (2011).
- 784 52. O. Levy, C. E. Ooi, J. Weiss, R. I. Lehrer, P. Elsbach, Individual and synergistic
785 effects of rabbit granulocyte proteins on *Escherichia coli*. *J Clin Invest* **94**, 672-
786 682 (1994).
- 787 53. B. Loh, C. Grant, R. E. Hancock, Use of the fluorescent probe 1-N-
788 phenyl-naphthylamine to study the interactions of aminoglycoside antibiotics with
789 the outer membrane of *Pseudomonas aeruginosa*. *Antimicrob Agents Chemother*
790 **26**, 546-551 (1984).
- 791 54. P. N. Paradkar, L. Trinidad, R. Voysey, J. B. Duchemin, P. J. Walker, Secreted
792 Vago restricts West Nile virus infection in *Culex* mosquito cells by activating the

- 793 Jak-STAT pathway. *Proceedings of the National Academy of Sciences of the*
794 *United States of America* **109**, 18915-18920 (2012).
- 795 55. T. J. Green, P. Speck, Antiviral Defense and Innate Immune Memory in the
796 Oyster. *Viruses* **10** (2018).
- 797 56. A. Woznica *et al.*, STING mediates immune responses in a unicellular
798 choanoflagellate. *bioRxiv* (2021).
- 799 57. D. L. Burdette *et al.*, STING is a direct innate immune sensor of cyclic di-GMP.
800 *Nature* **478**, 515-518 (2011).
- 801 58. D. Zhu *et al.*, Structural biochemistry of a *Vibrio cholerae* dinucleotide cyclase
802 reveals cyclase activity regulation by folates. *Molecular cell* **55**, 931-937 (2014).
- 803 59. D. J. Stefanik, L. E. Friedman, J. R. Finnerty, Collecting, rearing, spawning and
804 inducing regeneration of the starlet sea anemone, *Nematostella vectensis*. *Nat*
805 *Protoc* **8**, 916-923 (2013).
- 806 60. A. Karabulut, S. He, C. Y. Chen, S. A. McKinney, M. C. Gibson, Electroporation
807 of short hairpin RNAs for rapid and efficient gene knockdown in the starlet sea
808 anemone, *Nematostella vectensis*. *Developmental biology* **448**, 7-15 (2019).
- 809 61. M. J. Layden, E. Rottinger, F. S. Wolenski, T. D. Gilmore, M. Q. Martindale,
810 Microinjection of mRNA or morpholinos for reverse genetic analysis in the starlet
811 sea anemone, *Nematostella vectensis*. *Nat Protoc* **8**, 924-934 (2013).
- 812 62. F. S. Wolenski, M. J. Layden, M. Q. Martindale, T. D. Gilmore, J. R. Finnerty,
813 Characterizing the spatiotemporal expression of RNAs and proteins in the starlet
814 sea anemone, *Nematostella vectensis*. *Nat Protoc* **8**, 900-915 (2013).
- 815 63. D. I. Kotov, T. Pengo, J. S. Mitchell, M. J. Gastinger, M. K. Jenkins, Chrysalis: A
816 New Method for High-Throughput Histo-Cytometry Analysis of Images and
817 Movies. *Journal of immunology* **202**, 300-308 (2019).
- 818

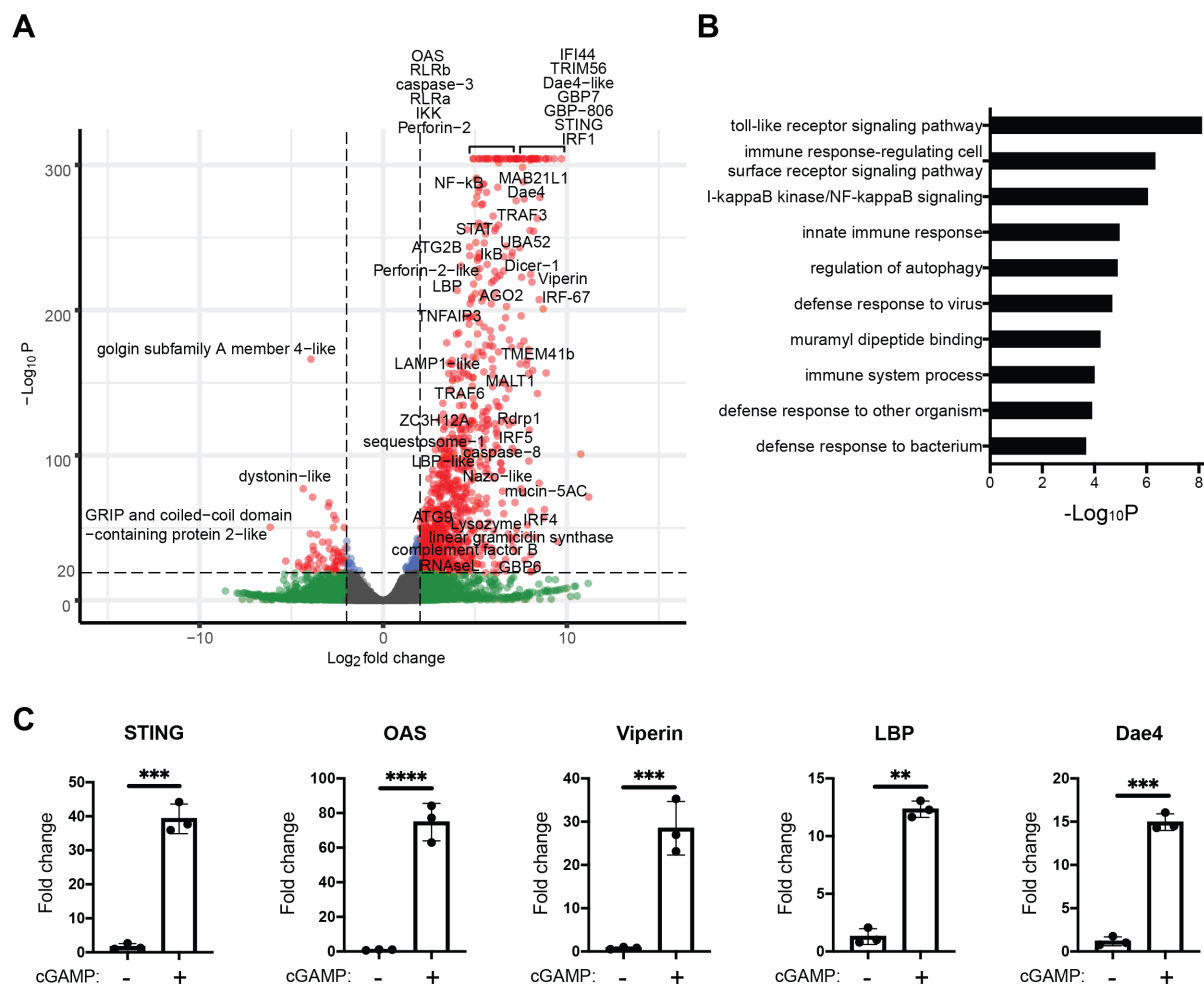


Figure 1: 2'3'-cGAMP induces many putative immune genes in *Nematostella vectensis*

- A) Volcano plot showing differential gene expression (DE) in *N. vectensis* polyps untreated vs. treated with 2'3'-cGAMP for 24 hours. A positive fold-change indicates higher expression in polyps treated with 2'3'-cGAMP. Genes of interest with homologs known to be involved in immunity in other organisms are labeled.
- B) Breakdown of DE genes into categories based on known GO terms. Gene set enrichment analysis shows a clear enrichment of GO terms associated with immunity.
- C) qRT-PCR measuring genes of interest in 48-hour-old *N. vectensis* embryos untreated or treated with 2'3'-cGAMP for 4 hours. Fold changes were calculated relative to untreated as $2^{-\Delta\Delta C_t}$ and each point represents one biological replicate. Unpaired t test performed on $\Delta\Delta C_t$ before log transformation. *p ≤ 0.05; **p ≤ 0.01; ***p ≤ 0.001; ****p ≤ 0.0001.

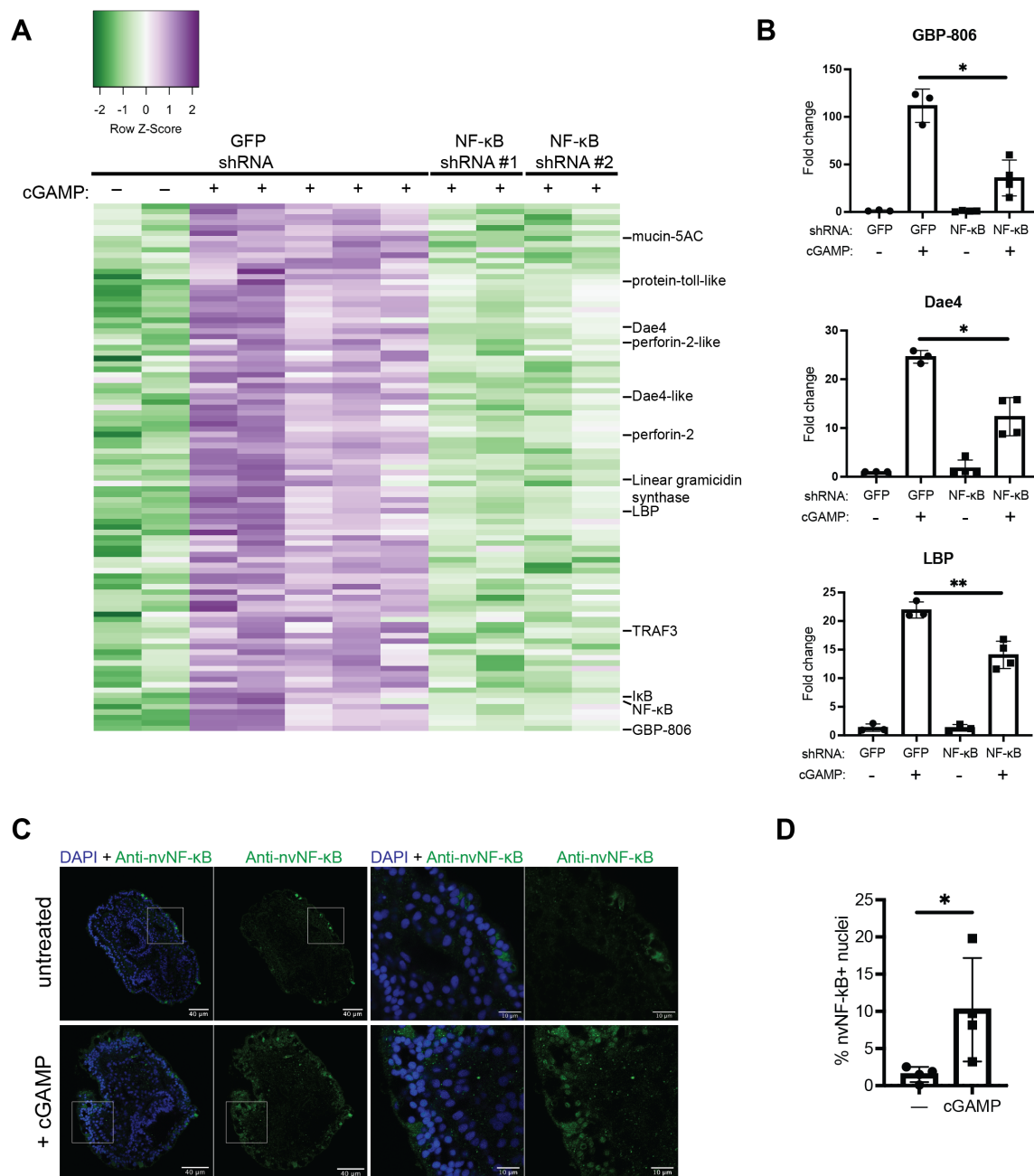


Figure 2: The induction of many anti-bacterial genes by 2'3'-cGAMP is nvNF-κB dependent

- A) Heatmap showing all genes that are significantly ($p_{adj} < 0.05$, $\log_2FC < -1$) downregulated in 2'3'-cGAMP -treated embryos microinjected with NF-κB shRNA vs. GFP shRNA. Genes with predicted antibacterial function are labeled
- B) qRT-PCR of antibacterial genes in nvNF-κB shRNA or control GFP shRNA treated samples after induction by 2'3'-cGAMP. Fold change was calculated relative to untreated, GFP shRNA injected as $2^{-\Delta\Delta Ct}$ and each point represents

one biological replicate. Unpaired t test performed on $\Delta\Delta C_t$ before log transformation. * $p \leq 0.05$; ** $p \leq 0.01$.

- C) Whole mount immunofluorescence of polyps stained with anti-nvNF- κ B antiserum. Right two panels are enlargements of the boxed regions indicated in the left two panels..
- D) Quantification of cells with nuclear localization of nvNF- κ B after treatment with cGAMP (representative images shown in C). Each point represents a single polyp, in which at least 1500 cells were analyzed. Statistical analysis was performed by unpaired t test; * $p = 0.0481$.

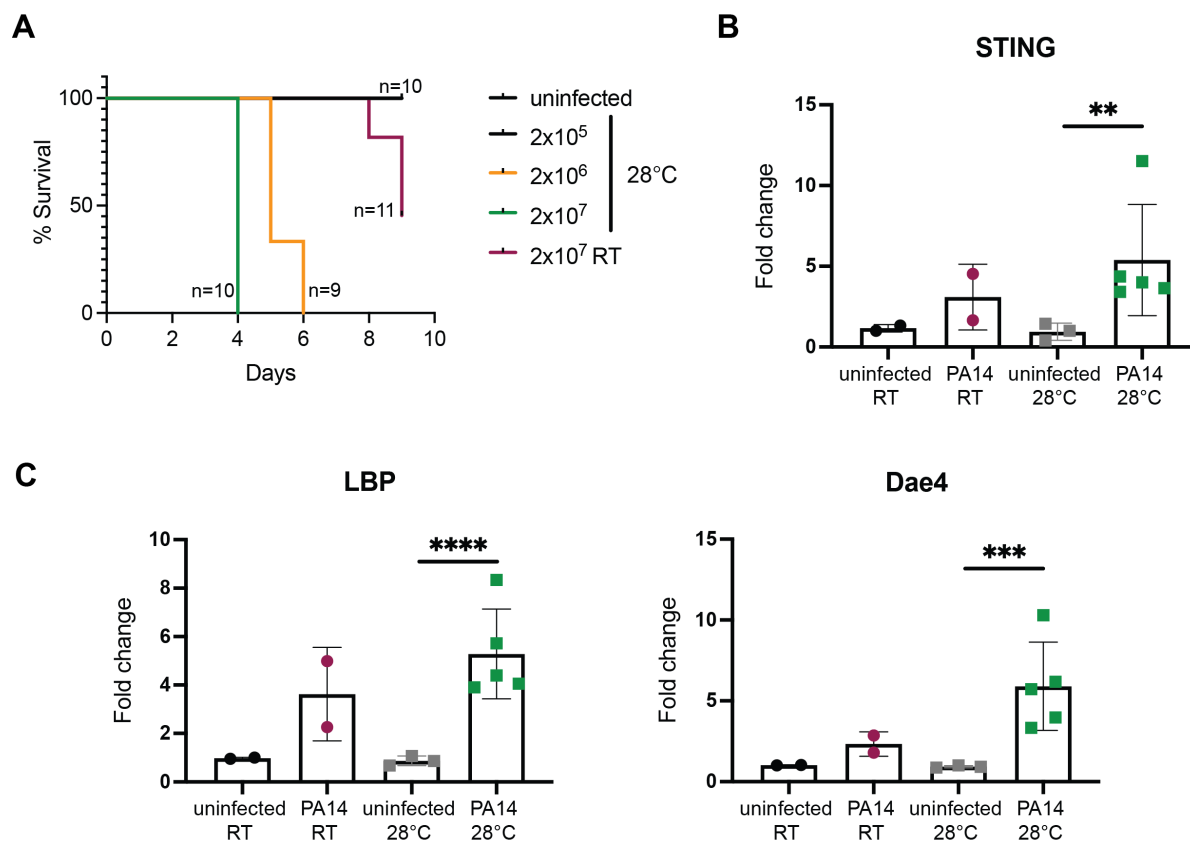


Figure 3: *Pseudomonas aeruginosa* infection induces putative anti-bacterial genes

A) Survival curves of *N. vectensis* polyps infected with *P. aeruginosa* at indicated dose and temperature.

B+C) qRT-PCR of nvSTING (B) or putative antibacterial genes (C) assayed at 48 hours post *Pa* infection (2×10^7 CFU/ml). Each point represents one biological replicate; unpaired t test performed on $\Delta\Delta Ct$ before log transformation. ** $p \leq 0.01$; *** $p \leq 0.001$; **** $p \leq 0.0001$.

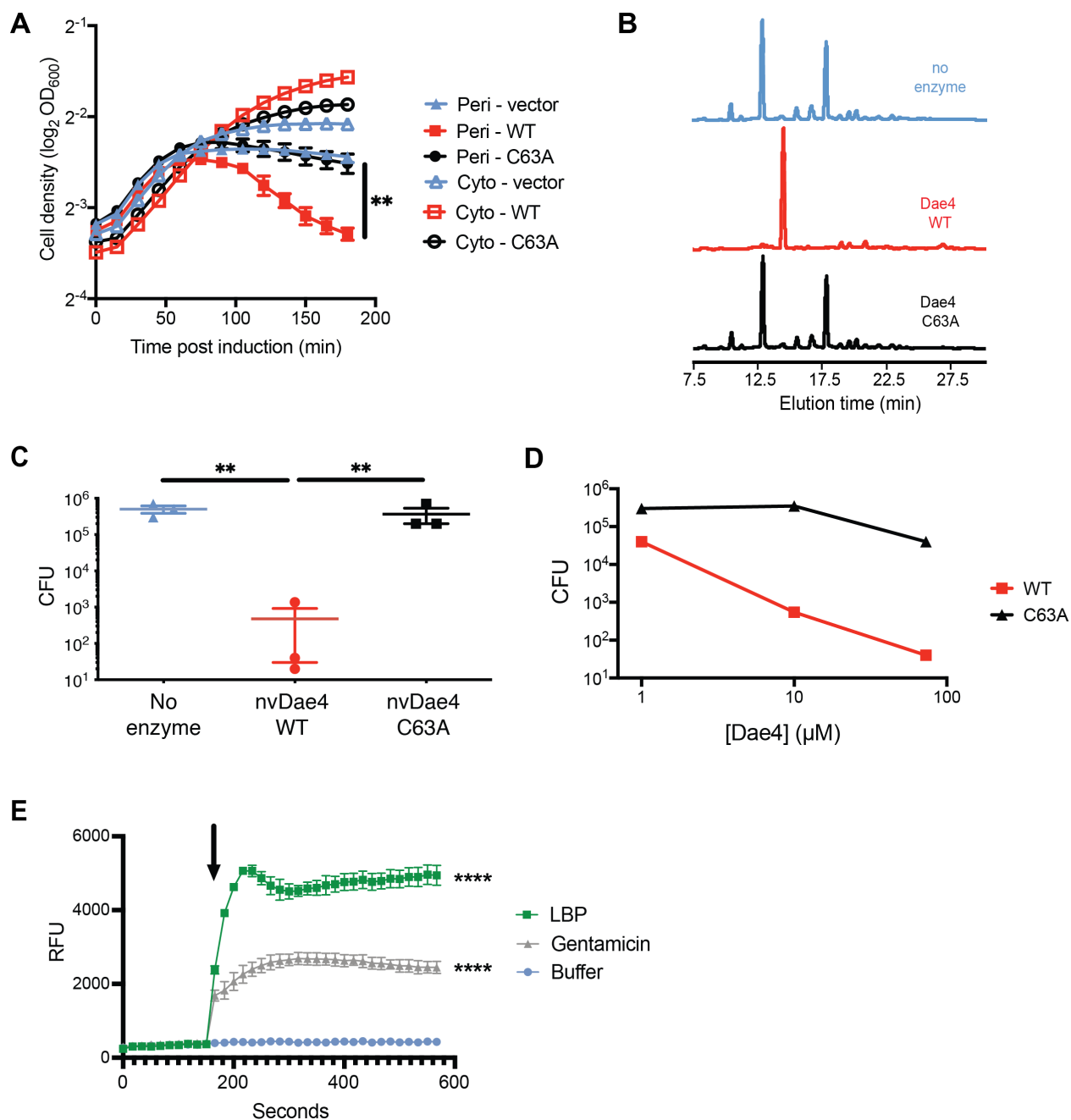


Figure 4: 2'3'-cGAMP induced, nvNF- κ B-dependent proteins have anti-bacterial activity

- A) Growth of *E. coli* expressing either periplasmic (Peri-) or cytosolic (Cyto-) nvDae4 (WT or C63A) induced with 250 μM IPTG. Error bars \pm SD; n=3. Unpaired t test; **p = 0.0063.
- B) Partial HPLC chromatograms of *E. coli* peptidoglycan sacculi after overnight incubation with buffer only (no enzyme), or 1 μM nvDae4 WT or C63A enzyme.
- C) *Bacillus subtilis* CFU after 2 hour incubation with buffer alone, nvDae4 WT or catalytic mutant C63A (25 μM). Error bars \pm SEM; n=3. Unpaired t test performed on log-transformed values; **p \leq 0.01.

- D) Dose dependent killing of *B. subtilis* by WT nvDae4 enzyme (same assay as in C).
- E) Fluorescence of *P. aeruginosa* (uptake of NPN) after treatment with nvLBP (4.5 μ M) or gentamicin (20 μ g/mL). Arrow indicates time gentamicin or nvLBP was added. Unpaired t test ; **** $p \leq 0.0001$.

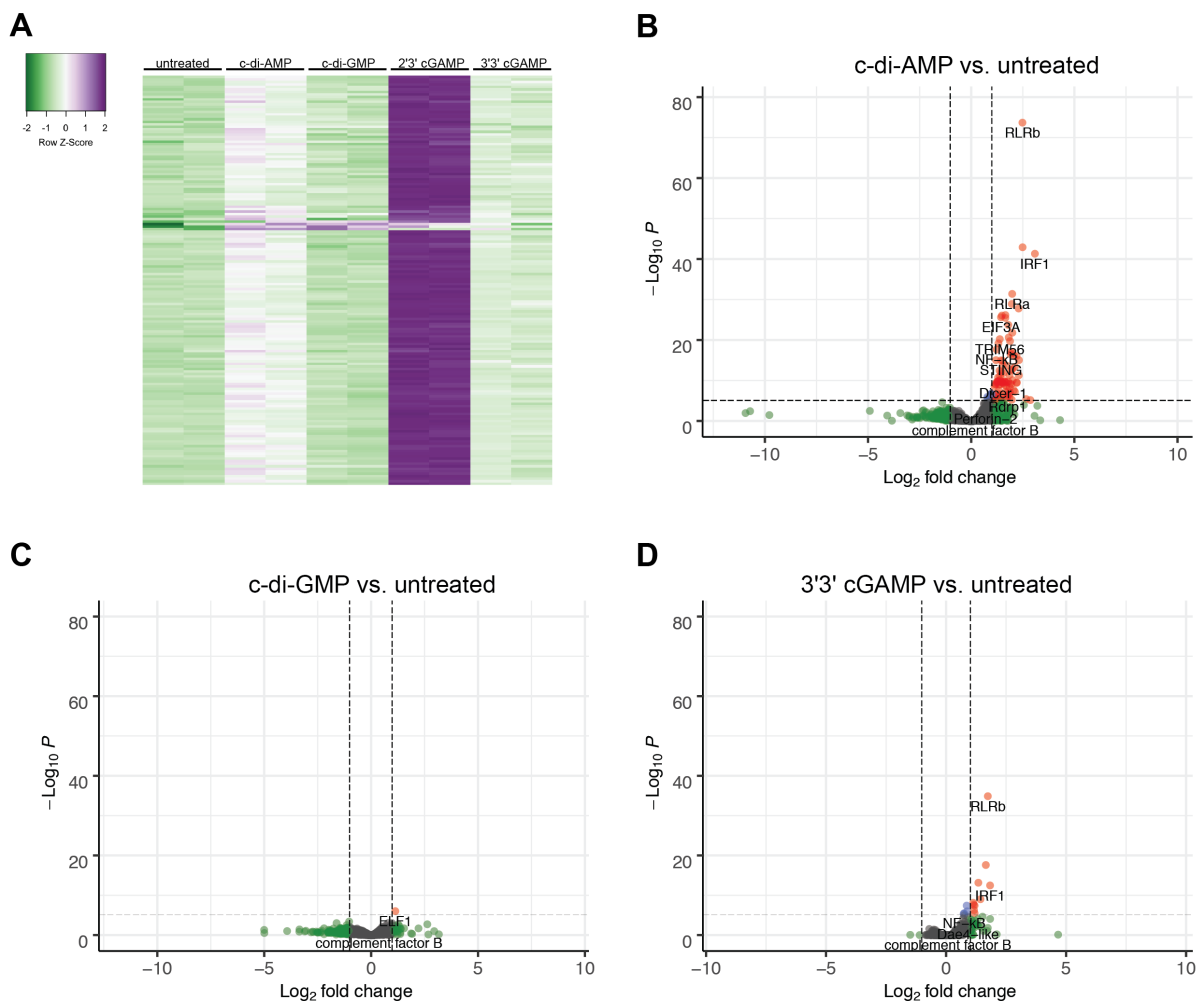


Figure S1: Treatment with other CDNs leads to some gene induction

A) Heatmap showing differentially expressed genes in response to c-di-AMP, c-di-GMP, and 3'3'-cGAMP. Almost all of these are also significantly induced by 2'3'-cGAMP.

B-D) Volcano plots of differential gene expression in *N. vectensis* polyps untreated vs. treated with cyclic-di-AMP (B), cyclic-di-GMP (C) and 3'3'-cGAMP (D) for 24 hours.

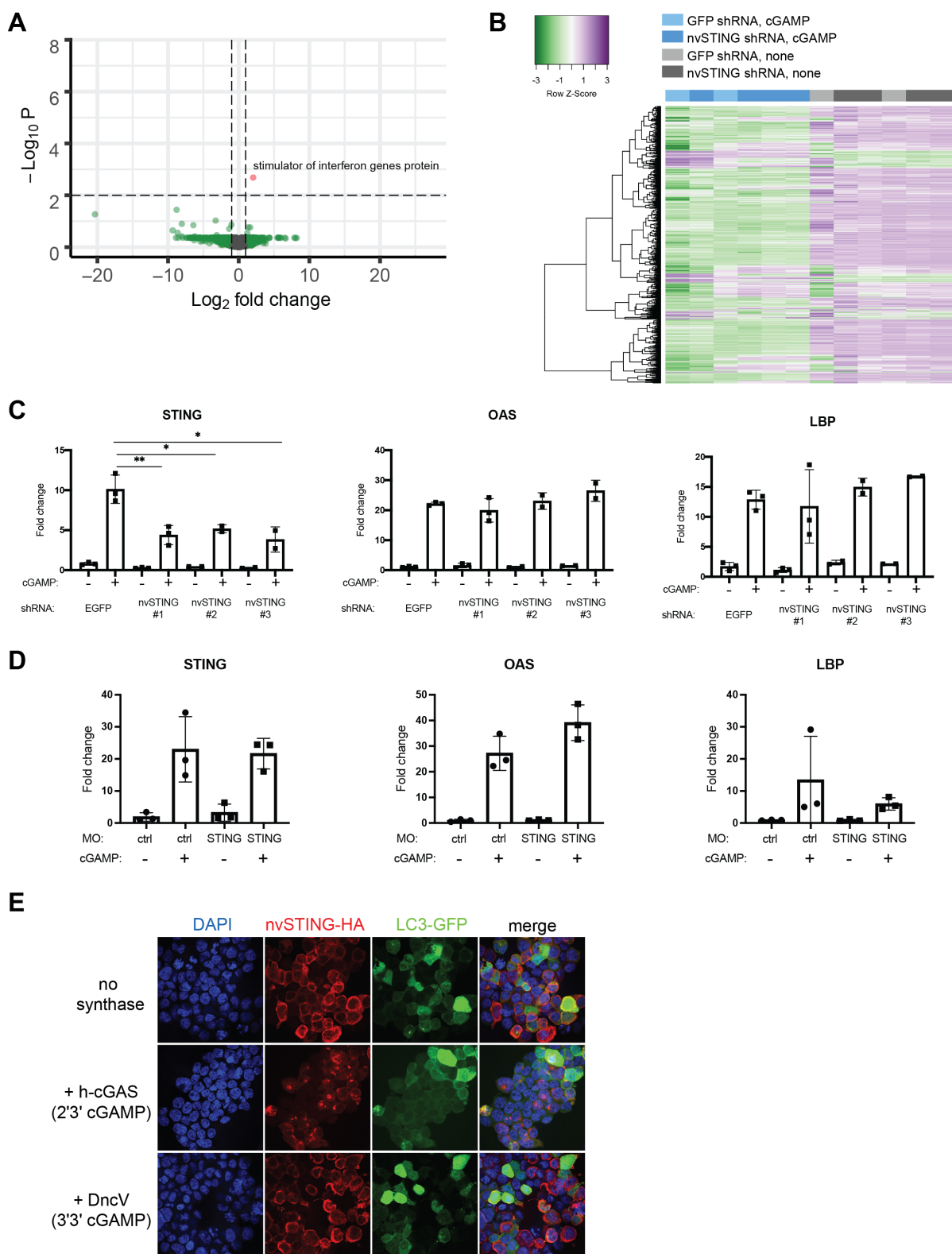


Figure S2: nvSTING knockdown does not impact the induction of genes by 2'3'-cGAMP

- A) Volcano plot showing differential gene expression in 48 hour embryos treated with 2'3'-cGAMP that were injected with GFP shRNA or nvSTING shRNA. Positive fold-change indicates higher expression in GFP shRNA injected embryos.
- B) Clustered heatmap showing the expression of the top 1000 varied genes by RNA-Seq between embryos injected with either GFP or nvSTING shRNA and either untreated or treated with 2'3'-cGAMP.
- C) Fold change of nvSTING, nvOAS, and nvLBP assayed by Nanostring from experiments using 3 different shRNAs to knock down nvSTING expression.
- D) qRT-qPCR measuring genes of interest in 48-hour-old embryos injected with a control (ctrl) or nvSTING translation-inhibiting morpholino (MO) and treated with 2'3'-cGAMP. Fold changes were calculated as $2^{-\Delta\Delta Ct}$ and each point represents one biological replicate. Unpaired t test performed on $\Delta\Delta Ct$ before log transformation; no significant differences.
- E) Immunofluorescence images of 293T cells transfected with plasmids encoding nvSTING-HA, LC3-GFP, and either empty vector, human cGAS or *V. cholera* DncV. Human cGAS is activated by the transfected DNA to produce 2'3'-cGAMP, and DncV, which produces 3'3'-cGAMP, is constitutively active in 293T cells.

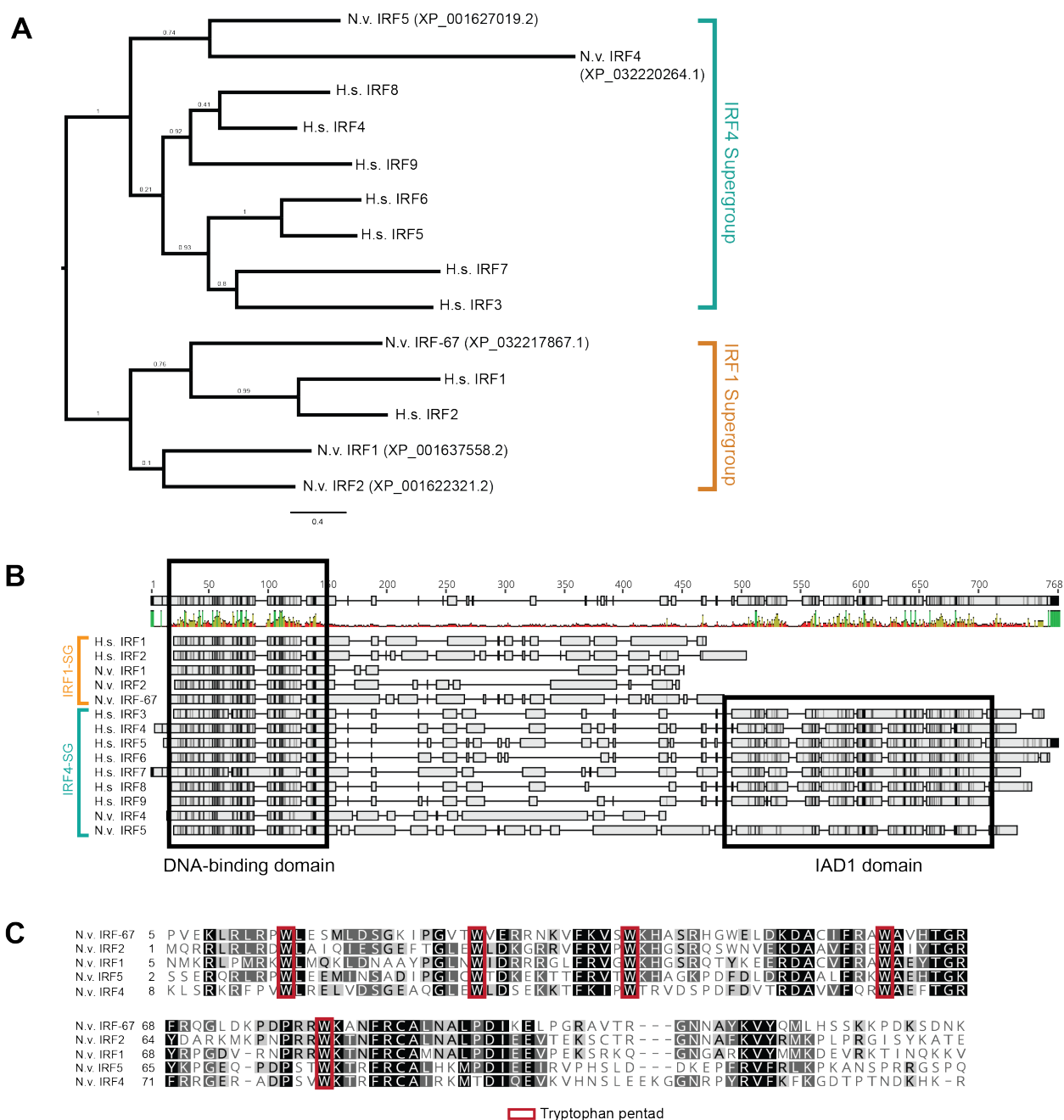


Figure S3: Phylogenetic study of *N. vectensis* IRFs

- A) Phylogenetic tree of all human and *N. vectensis* IRF proteins. 3 nvIRFs cluster with members of the human IRF1 supergroup, while the other 2 nvIRFs cluster with the IRF4 supergroup.
- B) Full protein alignment of sequences in A). The DNA-binding domain is highly conserved between all *N. vectensis* and human IRFs. Only nvIRF5 contains an IAD1 domain.
- C) Alignment of all nvIRF DNA-binding domains with conserved tryptophan pentad outlined in red

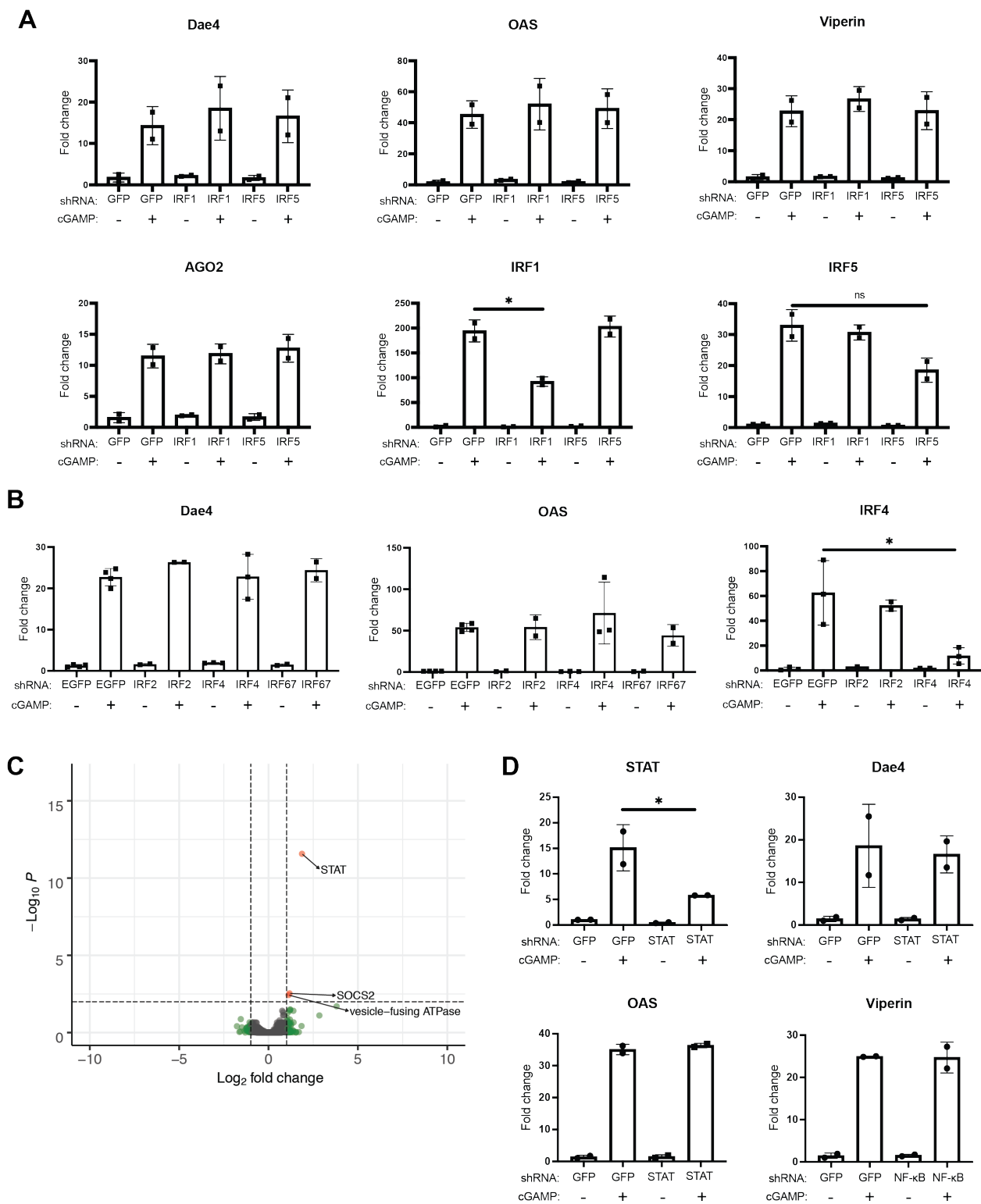
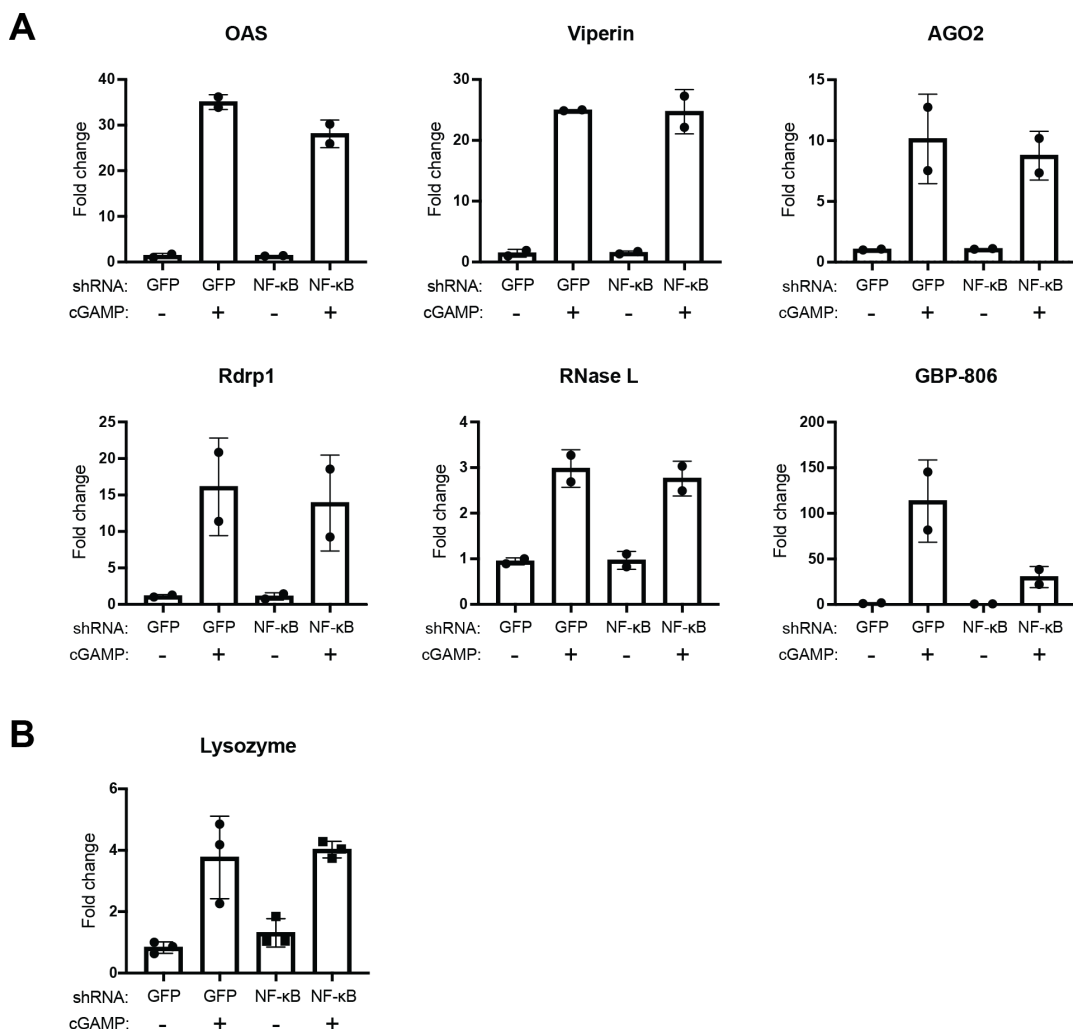


Figure S4: Knockdowns of nvIRFs or nvSTAT have no effect on 2'3'-cGAMP-induced gene expression

- A) Fold changes in gene expression as determined by Nanostring in embryos microinjected with shRNAs targeting EGFP, nvIRF1, or nvIRF5 either untreated or treated with 2'3'-cGAMP.
- B) Fold changes in gene expression as determined by qRT-PCR in samples microinjected with shRNAs targeting EGFP, nvIRF2, nvIRF-67, or nvIRF4 either untreated or treated with 2'3'-cGAMP. Note that IRF2 is not induced by cGAMP and was mostly undetected in all samples; therefore it is possible that the knockdowns were unsuccessful.
- C) Volcano plot showing differential gene expression as determined by RNA-Seq in 48 hour embryos treated with 2'3'-cGAMP that were injected with GFP shRNA or nvSTAT shRNA. Positive fold-change indicates higher expression in GFP shRNA injected embryos. The GFP shRNA samples here are the same as those shown in Figure 2A.
- D) Fold changes in gene expression as determined by Nanostring in embryos microinjected with shRNAs targeting EGFP or nvSTAT either untreated or treated with 2'3'-cGAMP.



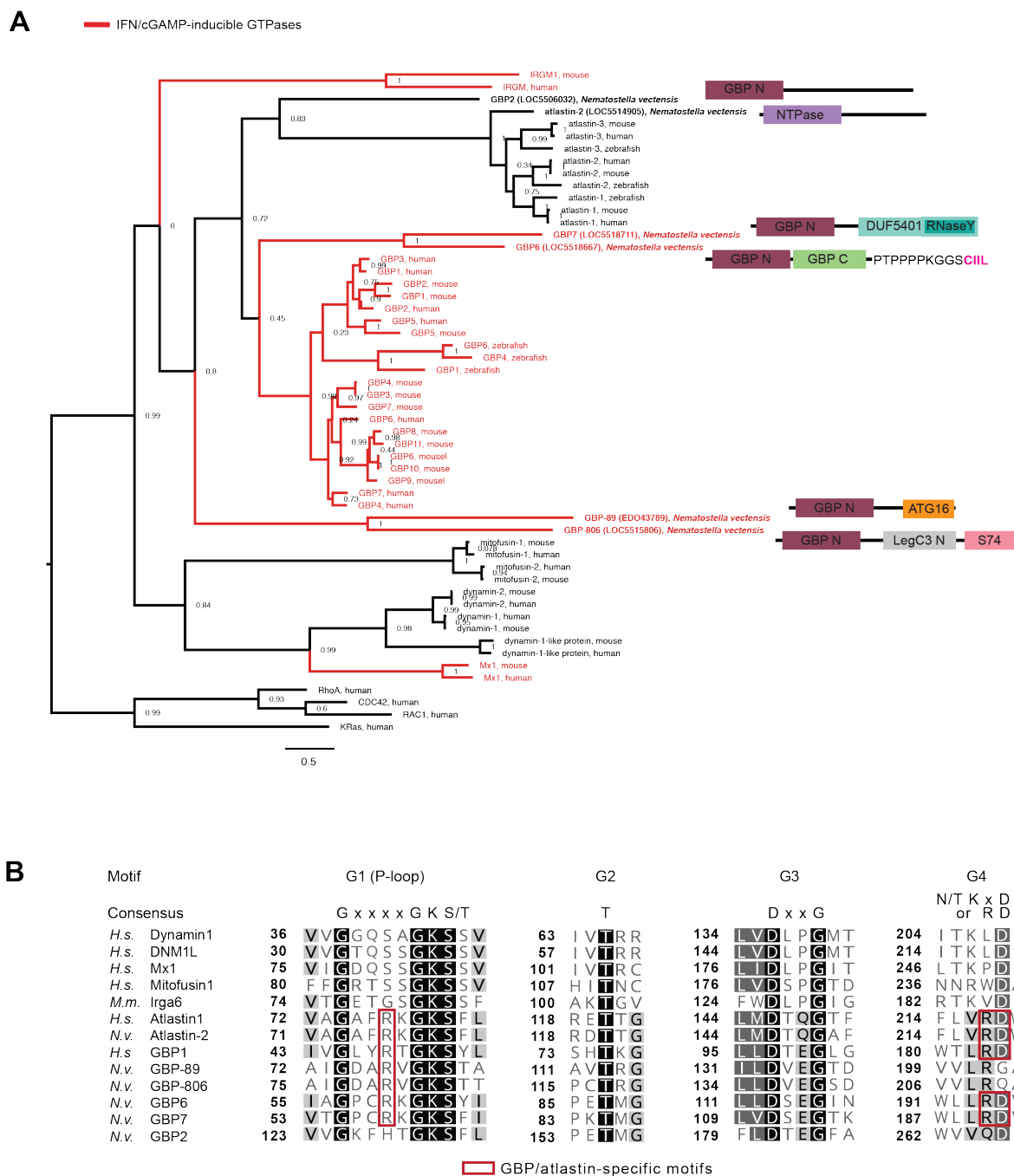


Figure S6: Phylogenetic study of *N. vectensis* GBPs

- A) Phylogenetic tree of mammalian GTPases and putative *N. vectensis* GBPs made with the full protein sequences. Branches with mammalian interferon-induced GTPases and cGAMP-induced *N. vectensis* GBPs are colored red; these tend to cluster together. Domain structures of *N. vectensis* GBPs are displayed.
- B) Alignment of the GTPase domains of all *N. vectensis* GBPs and select mammalian GTPase. Conserved GBP and atlastin specific residues are highlighted in red.

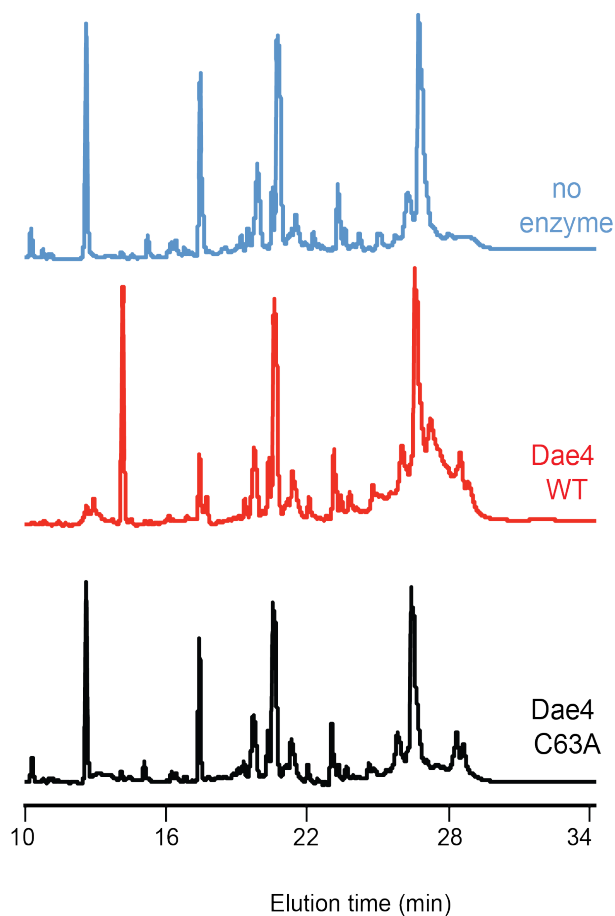


Figure S7: nvDae4 cleaves peptidoglycan from Gram-positive bacteria. Partial HPLC chromatograms of *Staphylococcus epidermidis* peptidoglycan sacculi products resulting from incubation with buffer only (no enzyme), or 1 μ M nvDae4 WT or C63A enzyme.

Table S1: Cnidarian-specific genes that are induced by 2'3'-cGAMP in an ν NF- κ B-dependent manner

NCBI Gene ID	Domains	Only in Cnidaria?	Only in Anthozoa?	Homolog found in immune cells in <i>Stylophora pistillata</i> (1)?
5501851	none	yes	yes	no
5504224	MDN1 super family	yes	yes	no
5516219	none	yes	yes	no
5516219	none	yes	yes	no
5518710	none	yes	yes	no
116603205	none	yes	yes	No homolog in <i>Stylophora pistillata</i>
116603727	none	yes	yes	No homolog in <i>Stylophora pistillata</i>
116604070	none	yes; except Bacillus spore coat proteins	yes; except Bacillus spore coat proteins	No homolog in <i>Stylophora pistillata</i>
116604505	none	yes	yes	No homolog in <i>Stylophora pistillata</i>
116612667	none	yes	yes	no
116613998	none	yes	yes	no
116616875	none	yes	yes; similar to 116620239	No homolog in <i>Stylophora pistillata</i>
116619128	none	yes	no	yes
116620239	none	yes	yes; similar to 116616875	No homolog in <i>Stylophora pistillata</i>

1. S. Levy *et al.*, A stony coral cell atlas illuminates the molecular and cellular basis of coral symbiosis, calcification, and immunity. *Cell* 10.1016/j.cell.2021.04.005 (2021).